Influence of Relative Humidity on the Stress Relaxation of Sucrose Compacts

William X. Guo

A thesis submitted in conformity with the requirements for the

Degree of Master of Science

Graduate Department of Pharmacy

University of Toronto

Influence of Relative Humidity on Stress Relaxation of Sucrose Compacts

William X.Guo

A thesis submitted in conformity with the requirements for the
Degree of Master of Science
Graduate Department of Pharmacy
University of Toronto

Abstract

Deformation kinetic analysis was used previously to develop a model to predict the viscoelastic deformation behavior of compacts composed of ductile material. This project was undertaken to extend and develop this model to evaluate the deformation kinetics of brittle pharmaceutical materials at various relative humidities. The effects of moisture on the deformation process are also hypothesized to be quantified by the same approach. Compacts were made from sucrose with various levels of pre-treated moisture content at compaction pressures of 3.5 and 4.5 MPa. Deformation kinetics indicated that plastic deformation will occur when the combined effect of stress and thermal energy increases the energy of the atoms to the point that the barrier to deformation can be overcome. The study proved that the deformation barrier of sucrose was symmetrical at equilibrium with a single energy barrier at lower humidity environments (relative humidity no more than 55%). Furthermore, this study was complicated by the fact that the deformation mechanism of the brittle material sucrose at ambient condition as different from that of the ductile material (*i.e.*, NaCl and KBr) studied previously. A thorough investigation of the experimental results indicated that when the sucrose was compressed at ambient conditions (relative humidity beyond 67%), two energy barriers, combined in series, must be overcome before any final appreciable flow occurs. Two kinetic parameters, the activation energy and activation volume, were calculated from the experimental data.

KEY WORDS: sucrose, tablet compaction, relative humidity, deformation kinetics, stress relaxation

ACKNOWLEDGMENTS

I gratefully acknowledge and express deep appreciation to the many wonderful people who have been instrumental in the completion of my work.

- to my supervisor Dr. Wendy C. Duncan-Hewitt for her patience, encouragement and guidance that allowed me to complete this thesis.

- my sincere thanks and appreciation to Dean Dr. D.G. Perrier for his understanding, encouragement and financial support during this Master program.

- to Dr. R.B. Macgregor, Dr. P.J. O'Brien and Dr. R.M. Pilliar for their administrative support, advice and encouragement.

- to Dr. Robert G. Miller and his colleagues of Ortho McNeil (Canada) Ltd for allowing and guiding me to use of equipment and the product development facility at Ortho McNeil.

- most of all, to my family, whose loving support has made this project possible.

TABLE OF CONTENTS

List of Tables

List of Figures

LIST OF ABBREVIATIONS

A, A_b,A_f:	frequency factor
A_j	the preexponential factor
a	parameter in brittle model
α	geometrical factor relating active slip system to shear strain direction
Af,b	activation frequency factor
b	Burgers vector
b	parameter in brittle model
c	crack length
d	distance, diameter
ΔE (f,b,e)	activation energies
E	elastic modulus
ε	strain
$\dot{\varepsilon}$	strain rate
$\dot{\varepsilon}_{shear}$	shear strain rate
F, F_c	force, contact force
H	Vickers hardness, MPa
h	crushed asperity height
K, K_b, K_f	rate constant; rate constant, backward and forward directions, respectively
k	Boltzmann constant, 1.36e-23 J K^{-1}
K_c	fracture toughness
k_H	slope of the Heckel plot
κ	the transmission coefficient
ν	Poisson ratio
P	load, N
θ	angle of rotation
R	radius of a reference cell
r	radius
RD, RD_i	relative density, initial relative density
ρ_m	mobile dislocation density
δ	the contribution to the deformation rate by each activation
ρ	the concentration of flow units (mobile dislocation density or vacancy concentration).

r_r	radius of a reference sphere
σ	stress
σ_{ct}	contact stress
S_f	free surface remaining on sphere
σ_f	fracture stress
σ_p	punch stress
T	absolute temperature, K
τ	shear stress
$\dot{\tau}$	shear stress rate
t	time
V_{act}	activation volume
V_{ex}	volume of material cut off by a face of the Voronoi cell
V_p	particle volume
V_r	volume of the reference cell
γ	shear strain
$\dot{\gamma}$	Shear strain rate
W_b, W_f	work performed in backward and forward directions respectively
Y	plastic yield stress
y	parameter in brittle model
Z, Z_i	coordination number
Z_r	recovered depth of indentation

Definition of Some Engineering Terms

The terms below are chosen because of their relation to the mechanical tests in this project (Hertzberg, 1976; Krausz and Eyring, 1975; Papadimitropoulos, 1990). An understanding of these terms is essential for development of the proposed model.

Brittle fracture: A specimen separates into two or more pieces after being subjected to a stress before appreciable plastic deformation or creep is observed.

Brittle material: A brittle material is one in which no plastic deformation occurs prior to fracture.

Compressibility of powders is the ability to decrease in volume under pressure.

Compactibility is the ability of the powdered material to be compressed into a tablet of specified tensile strength.

Compression test: Method for determining behavior of materials under crushing loads. Specimen is compressed, and deformation at various loads is recorded. Compressive stress and strain are calculated and plotted as a stress-strain diagram which is used to determine the elastic limit, proportional limit, yield point, yield strength and compression strength.

Creep: Deformation that occurs over a period of time when a material is subjected to constant stress at constant temperature.

Dashpot: A mechanical device which extends at a constant velocity when subjected to a constant force, and consists of a piston moving in a cylinder filled with a viscous fluid.

Deformation energy: Energy required to deform a material a specified amount. It is the area under the stress-strain diagram up to a specified strain.

Ductile material: A ductile material is one in which considerable amounts of plastic deformation can occur before it fractures.

Ductile fracture: Separation of material under plastic flow prior to rupture

Flow stress: Stress required to cause plastic deformation.

Hooke's law: Stress is directly proportional to strain. Hooke's law assumes perfectly elastic behavior. It does not take into account plastic or dynamic loss properties.

Kelvin or Voigt Model: A model which comprises a spring and dashpot connected in parallel is used to describe visco-elastic behaviour.

Plastic deformation: Deformation that remains after the load causing it is removed. It is the permanent part of the deformation beyond the elastic limit of a material.

Maxwell model: A model which comprises a spring and dashpot connected in series use to describe visco-elastic behaviour.

Stress rate: Change in stress with respect to time

Strain rate:Change in strain with respect to time

Shear strain rate: Change in shear strain with respect to time

Stress relaxation: Decrease in stress in a material subjected to prolonged constant strain at a constant temperature.

Stress-strain diagram: Graph of stress as a function of strain. It can be constructed from data obtained in any mechanical test where load is applied to a material, and continuous measurements of stress and strain are made simultaneously.

Viscoelasticity: Present when a deformed solid exhibits both viscous and elastic behavior through simultaneous dissipation and storage of mechanical energy. The ratio between dissipated and stored energy is rate (time) dependent.

CHAPTER ONE INTRODUCTION AND OVERVIEW

1.1. PURPOSE OF THIS STUDY

Tablet compaction is a complex process that is affected by many factors that are intrinsic to a formulation, such as composition and granulation methodology and by extrinsic factors such as the temperature, rate of compaction and humidity. The latter factor, humidity, can affect the characteristics of a compact to a startling degree. For example, varying the humidity can create a product that is excessively hard, friable or soft. A change in moisture content can cause a product that is compacted successfully under normal conditions to cap or laminate (Fig. 1.1.1) during decompression or ejection. Since tablets continue to be the most widely used drug delivery system in medicine today, there is a considerable economic incentive to investigate and solve these problems.

Although the foregoing is common knowledge, quantitative data concerning the role of moisture in compaction is scarce. The research described in this thesis was undertaken to elucidate some aspects of the role of moisture in compaction. In particular, the role of moisture in the single crystal microindentation behaviour and the deformation kinetic analyses of stress relaxation were used to explore the effects of water on the kinetics of sucrose crystal deformation during compaction.

1.1.1. Introduction of Model Material Sucrose

This project is concerned with sucrose crystals (Fig. 1.1.2), a disaccharide ($C_{12}H_{20}O_{11}$, ß-D-fructofuranosyl-∂-D-glucopyranoside), possessing a molecular weight of

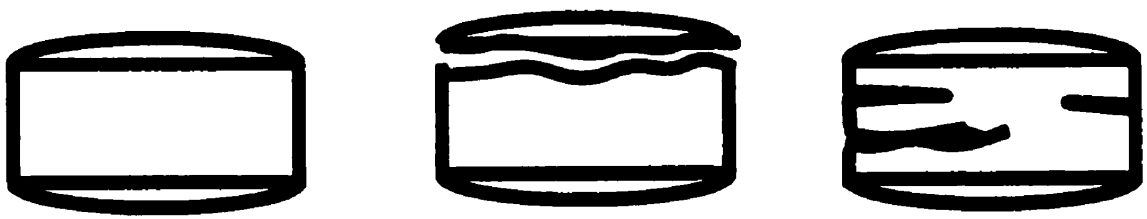

Fig. 1.1.1 Capping is separation of the top or bottom from the main body of the tablet. Laminating is transverse cracking and separation of the tablet into two or more layers.

342.30 (Grayson, 1983). Sucrose was chosen as model material for the following reasons:

1. Sucrose is widely used in the pharmaceutical industry when producing tablets both as a filler and a binder.
2. Sucrose is noted for its ability to adsorb and absorb water. Sucrose possesses a high affinity for water. One gram of sucrose crystals can dissolve in 0.5ml water at 25°C (Windholz *et al.*, 1983).
3. Sucrose is a large, asymmetric, organic crystalline compound. It is typical of many pharmaceuticals possessing numerous intermolecular hydrogen bonds in the crystalline state.
4. Some studies related to the properties of sucrose have been carried out in our group, so that it is already familiar to us.

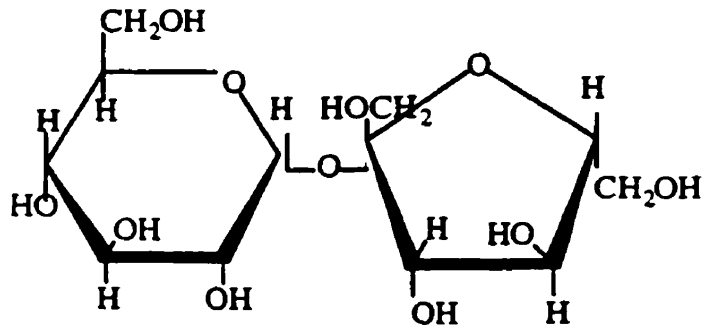

Fig. (1.1.2). Structural formula of sucrose (ß-D-Fructofuranosyl-*a*-D-glucopyranoside)

1.1.1.1. *Crystal structure*

Sucrose not only crystallizes in an anhydrous form under normal conditions but also forms a hemipentahydrate, a hemiheptahdrate, and several other unidentified forms (Young and Jones, 1948). Anhydrous sucrose crystals are monoclinic and hemimorphic (Brown and Levy, 1963). The fine structure of anhydrous sucrose crystals has been studied using both X-ray diffraction (Beevers *et al.*, 1952) and neutron diffraction (Brown

and Levy, 1963). The dimensions of the unit cell (nm) are a:b:c=1.0864:0.8704:0.7758 and its volume is 0.71504 nm^3. Each unit cell contains two sucrose molecules.

Each asymmetric unit possesses seven hydrogen bonds, two of which are intramolecular. Packing is determined essentially by hydrogen-bonding of the hydroxyl groups of the furanose residues. Sucrose possesses an enthalpy of crystallization of -415.98 $jmol^{-1}$ (from melt), an enthalpy of formation of 360 j mol^{-1}, and its enthalpy of solution in water is 5.523 kj mol^{-1} (Washburn, 1926; Duncan-Hewitt, 1989).

1.1.1.2. *Water Vapour Sorption of Sucrose*

The strong interactions between water and sucrose molecules leads to high solubility and sucrose may be hydrated with up to four molecules of water in solution. Large amounts of intracrystalline water are accommodated by the sucrose crystal (0.001 to 0.4%), which is probably retained within the dislocation cores (Thomas and Williams, 1967, Duncan-Hewitt, 1989).

Sucrose begins to dissolve in water which is adsorbed to the surface of the crystal when it exposed at or above r.h. 84.3% (Van Campen *et al.*, 1983b). The surface of the crystal then becomes coated with progressively thicker layers of its saturated solution (Panacoast and Junk, 1980). Water molecules diffuse into the crystal, and the sucrose molecules become more mobile. Exposure of sucrose crystals to air which was saturated with water at 25°C (100% r.h.) caused a linear increase in the weight of sucrose crystals ($9.6 \cdot 10^{-4}$ mg/s cm^2. Van Campen *et al.*, 1983a).

Sucrose (Power and Dye, 1966; Hüttenrauch, 1977) can take up relatively large

amounts of water below critical relative humidity and can form metastable solutions which recrystallize on standing or with drying.

1.1.1.3. *Mechanical Behaviour*

The hardness of sucrose crystals ranges from 470 MPa (Gebler and Bauer, 1984) to about 630 MPa (Ridgway K., Shotton, E and Glasby, 1970 636MPa; Aulton, 1977 624 MPa). The low values possibly arise from the effect of water trapped within the larger crystals. Duncan-Hewitt and Weatherly, 1989 used microindentation techniques to evaluate fracture toughness and deformation kinetics of sucrose crystals. Its fracture behavior was reported to be brittle and its deformation kinetics resemble those of ice, the crystal lattice of which is highly hydrogen-bonded, similar to that of sucrose.

1.2. HYPOTHESIS

The analysis of the stress relaxation of tablets composed of the ductile materials NaCl and KBr (Papadimitropoulous and Duncan-Hewitt, 1992) using deformation kinetic theory yielded estimates of activation energy and activation volume that were indistinguishable, statistically, from values obtained by more conventional means (Frost and Ashby, 1982). In the present study we hypothesized that this approach could be extended to the evaluation of the kinetics of a brittle material, sucrose. Furthermore moisture is known to play a significant role in the deformation of sucrose. It was also hypothesized that the effect of moisture might be quantified by the same approach.

We study of that water can both greatly facilitate viscous deformation by acting as

an intermediary during the process of bond breaking and formation, and may also assist in the formation of stronger bonds through hydrogen bonding. The latter might increase interparticulate friction, making densification more difficult but might also increase tablet strength. Depending upon the exact mechanisms involved, it might be possible to quantify these effects by deformation kinetics analysis.

1.3. OBJECTIVE

The primary objective of this project was to investigate the influence of moisture on the mechanical behavior of sucrose tablets during the stress relaxation stage using deformation kinetic analysis.

1.4. BACKGROUND TO PHARMACEUTICAL MATERIALS TECHNOLOGY

1.4.1. Mechanical Behaviour of Materials

The influence of moisture on pharmaceutical powder compaction is complex because conceivably, it could affect every mechanism that gives rise to densification. When a powder is compressed, the particles will undergo rearrangement, reversible (elastic) and irreversible (plastic or viscous) deformation and fracture.

1.4.1.1 *Elastic Deformation*

Elastic deformation can be defined as time-independent deformation which

disappears (at the speed of sound) once the load applied to a material is released. Viewed at a microscopic level at equilibrium, atoms in condensed phases occupy equilibrium positions although they may be vibrating about the minimum of the free energy wells. When a force causing a stress below the yield point is applied, the atoms are displaced elastically from their equilibrium positions. The potential energy of the system is increased and stored in a reversible manner. If the body is perfectly elastic, the atoms return spontaneously to their original equilibrium configuration as the stress is removed and a corresponding quantity of energy is released (Krausz and Eyring, 1975).

The deformation or strain of an elastic body under load is dependent only upon the final stress and not upon the stress history or strain path. Therefore, elastic behaviour may be viewed as a point function since any induced strain can be determined from the initial and final stress and appropriate proportionality constants (Caddell, 1980).

At low levels of strain, Hooke's law can be used to describe the relationship between stress and strain. Elastic behaviour is modeled by an ideal spring whose behaviour obeys (Hooke's law) the equation:

$$\sigma = E\varepsilon \qquad (1)$$

Where σ is the stress on the spring, ε is the strain, and E is the proportionality constant often called Young's modulus. In an elastic crystalline solid, the elastic constant depends on the shape of the potential field of the atoms or molecular units, and the configuration is nearly constant (Krausz and Eyring, 1975).

1.4.1.2. *Plastic Deformation*

Plastic deformation occurs when the elastic limit has been exceeded, and non-recoverable deformation occurs. In the absence of stress, random diffusion processes cause molecule rearrangement that does not give rise to any net strain. These processes are unbalanced and accelerate when stress is applied. Thus, during plastic deformation the atoms move under the combined effect of the applied stress and thermal excitation into a new equilibrium positions thus breaking previous bonds and establishing new ones (Krausz and Eyring, 1975). Movement of molecules can occur only adjacent to voids associated with surfaces, dislocations or vacancies.

To produce plastic deformation or flow, a certain level of stress, called the *yield stress*, must be exceeded. The deformation produced is largely irreversible and the final strain is found to depend upon the history of loading rather than on the initial and final stresses, i.e., plasticity is a path function (Caddell, 1980). True plasticity is independent of time so that the speed of load application does not influence the resultant deformation.

1.4.1.3 Viscoelasticity

The description of plasticity does not account for the time dependence that is not observed in most real deforming systems. Furthermore, true plastic deformation demands a minimum stress level or elastic limit to be exceeded, whereas in reality any amount of applied stress will cause permanent deformation, although the amount may be negligible unless sufficient deformation time is allowed. Both of these observations may be accounted for by so-called viscous effects (Caddell, 1980). In its *linear* form, viscous flow is defined as Newtonian flow for which the rate of strain is directly proportional to

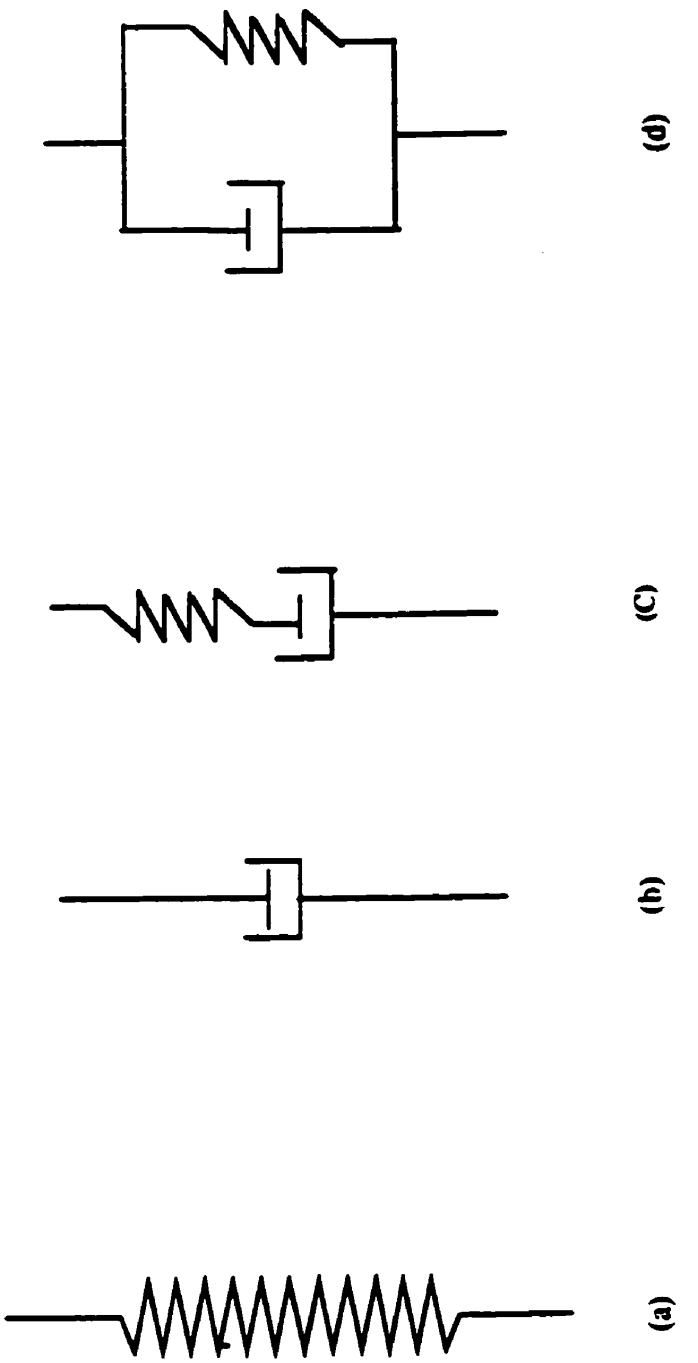

Figure 1.4.1.3.1 Two elements used in mechanical models of viscoelasticity: (a) spring (b) dashpot, (c) The Maxwell unit consisting of a spring and a dashpot in series. (d) Kelvin solid consisting of a spring and a dashpot in parallel (Krausz and Eyring, 1975)

the applied stress (Rippie and Danielson, 1981).

Linear viscous behaviour is modeled by a linear dashpot (Fig 1.4.1.3.1) which can be visualized as a piston moving in a cylinder lubricated by a viscous material. A stress is required to displace the piston. This dashpot's behaviour obeys the equation:

$$\sigma = F\frac{d\varepsilon}{dt} \qquad (2)$$

Where $\frac{d\varepsilon}{dt}$ is the strain rate, and F is the viscous proportionality constant.

At a molecular level, some molecules are too firmly bonded to slip. These act as pure springs, and their behaviour is described by elasticity theory. Other molecules, not so firmly bonded, can move past each other, and act as viscoelastic units. Viscoelastic deformation is a combination of both elastic (time-independent) and viscous (time-dependent) components.

The spring and dashpot can be combined in a variety of ways to model viscoelastic behaviour. If a spring and a dashpot are combined in series, the modeled material is known as a Maxwell fluid (Fig.1.4.1.3.1) with mechanical behaviour described by the equation:

$$\frac{d\sigma}{dt} + \frac{E}{F}\sigma = E\frac{d\varepsilon}{dt} \qquad (3)$$

Where $\frac{d\sigma}{dt}$ is the stress time derivative, and the other symbols are as defined above.

Under uniaxial tension, an instantaneous extension of the spring occurs. This is the

elastic (Hookean) response of the model. At the same time, the fluid in the dashpot passes slowly through an orifice in the piston resulting in an extension of the overall length of the dashpot. This is a viscous flow which is referred to as the 'time-dependent' response of the Maxwell model.

If the two elements are combined in parallel, the material is known as a Kelvin solid (Fig. 1.4.1.3.1) based on an equal strain of the two elements. Thus, the stress is distributed between them so that they have the equation:

$$\sigma = E\varepsilon + F\frac{d\varepsilon}{dt} \qquad (4)$$

When a Kelvin solid is subjected to a strain profile, the resultant stress will be a linear function of the magnitude of the strain and the strain rate. It will behave like a spring when strained slowly but when subjected to a large rate of strain, the behaviour of the dashpot will predominate.

More complicated models can be constructed by combining more of these two fundamental elements in series and/or parallel. For example, a three element linear viscoelastic model is composed of two Hookean springs and one Newtonian dashpot. However, the assumptions of linearity for the elements are often not justified in the investigation of the deformation behaviour of many materials, because the deformation is a thermally activated process.

Empirical studies have shown that most viscous materials can be can be represented with the Halsey-Eyring three-element model (Halsey, G. *et al.*, 1945) (Fig.1.4.1.3.2).

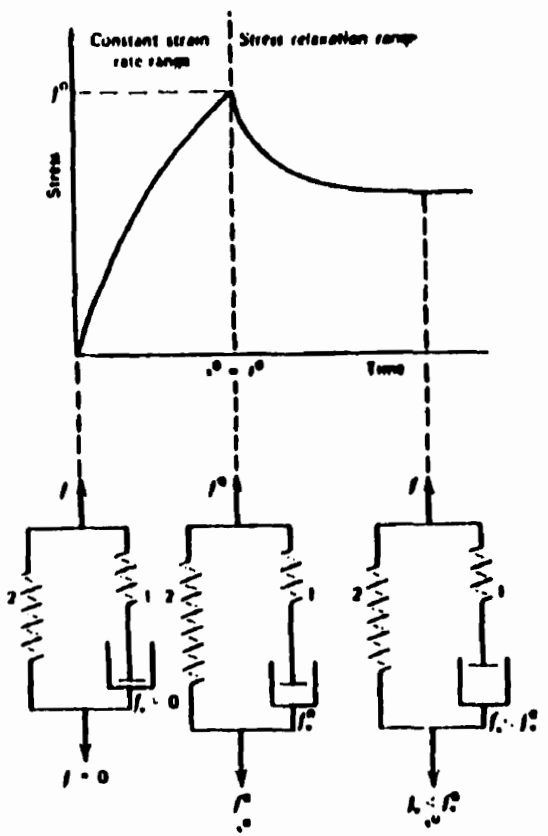

Maxwell unit

Spring , time independent elastic element

Dashpot, time-dependent element

The time dependent flow decreases the total stress as a function of time $f(t)=(f^{\circ}-f^{\circ}_{,})+f_{,}(t)$

f°: maximum stress while straining to s°

$f^{\circ}_{,}$: stress acting on spring 1 instantaneously while straining to s°

$f_{,}(t)$: time dependent stress acting on spring 1 which decreases as the dashpot slips

$(f^{\circ}-f^{\circ}_{,})$: stress acting on spring 2 which remains unchanged during stress relaxation.

Fig.1.4.1.3.2. Halsey-Eyring mechanical model illustrates the stress-time relation (Halsey, G., *et al.*, 1945)

1.4.1.4. *Fracture*

If the elastic limit is exceeded, and if the rate of application of the load is sufficiently rapid such that the material is incapable of deforming elastically and plastically at a rate sufficient to accommodate the induced stress, the material may fracture.

Fracture processes are generally studied at three separate levels: atomic, microscopic, and macroscopic. At the atomic level, bond-breaking processes are investigated. At the microscopic level, the laws of statistical mechanics, the chemical processes in the atomic structure of materials and the consequences of an imposed complex stress and strain field are considered. At the macroscopic level, the material is modeled as a continuum and the atomic and structural reality is smoothed out to facilitate the mathematical analysis of complex, large scale, occurrences (Krausz and Eyring, 1975).

Fracture may be categorized as brittle or ductile. With brittle fracture there is little if any permanent deformation and the shape changes are minimal. Ductile fracture, however, is preceded by appreciable plastic deformation before separation occurs. Most actual fractures involve both modes but are usually dominated by one. In a crystallographic sense, brittle fracture usually occur by cleavage, in which the tensile stresses literally pull apart adjacent planes of atoms. Ductile fracture usually occurs as a result of shear stresses that cause atoms to slip with respect to each other (Caddell, 1980).

Figure 1.4.1.4.1(a) describes the behaviour of brittle materials. The stress-strain curve shows that a limited amount of strain energy is stored in a specimen up to the onset of fracture. Although the fracture stress may be relatively high, very little energy is stored

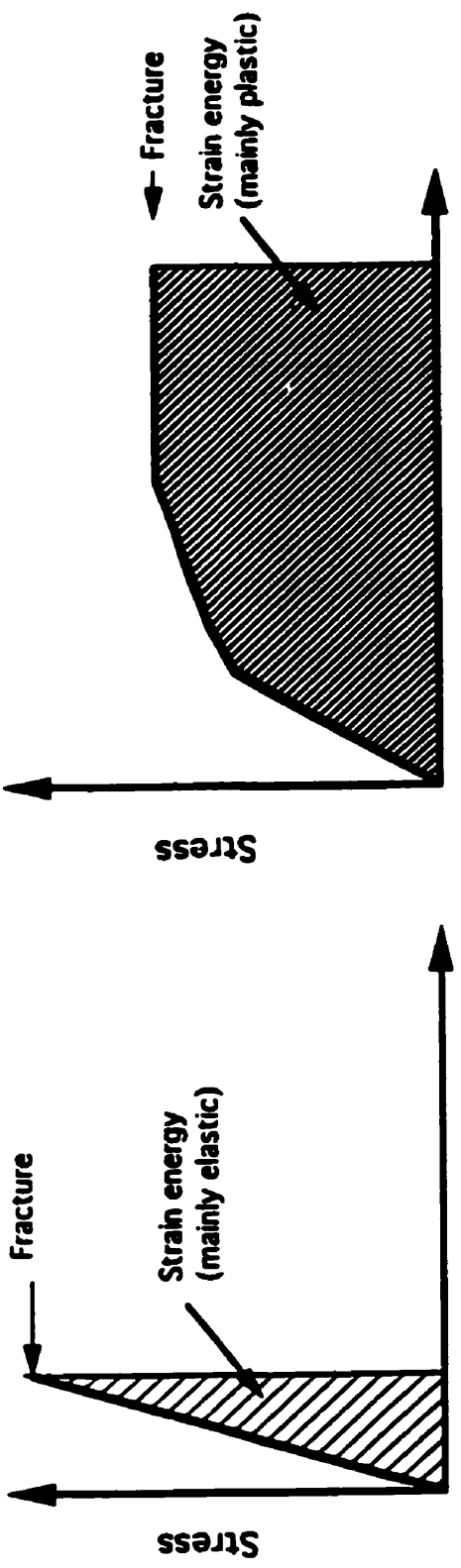

Fig.1.4.1.4.1. Stress-strain behavior of brittle solids (a) and ductile solids (b)

prior to failure. Figure 1.4.1.4.1(b) displays the behaviour of ductile materials such as lead or aluminum. A large reduction of area occurs and much larger amounts of irreversible strain energy are stored prior to fracture. As a rule, material or process factors that increase the slope of the stress-strain curve tend to increase the probability of brittle fracture in a normally ductile material.

Brittle fracture demands the existence of a crack or flaw somewhere in the solid, and stresses that induce the crack to propagate. According to the Griffith criterion (Griffith, 1920), a crack will propagate when the decrease in elastic strain energy is at least equal to the energy needed to create the new surfaces associated with the crack.

1.4.1.5. *Crystal Hardness*

Over recent years, studies of the hardness of single crystals of pharmaceutical materials have been undertaken to obtain a better picture of their deformation and bonding characteristics during tableting. In a recent typical example, Duncan-Hewitt *et al.*, (1994) classified acetaminophen as being semi-ductile using microindentation hardness.

i) Hardness Test

Crystal hardness can be defined as a measure of the resistance to local permanent deformation and is primarily related to plasticity. In a typical hardness test, a small, very hard, indenter is pressed into the surface being examined under a known load. The surface undergoes plastic deformation, and the indenter moves accordingly through a small distance to produce a permanent indentation. The group of tests will be described below

to emphasize the multifunctional nature of hardness.

Brinell Test:

The Brinell method (Figure 1.4.1.5.1) applies a predetermined test force (F) to a small sphere of fixed diameter (D) which is held for a predetermined time and then removed. The resulting indentation is measured across at least two diameters (d). The Brinell hardness number (BHN) is then calculated using the following equation:

$$BHN = \frac{2F}{\pi D(D - \sqrt{D^2 - d^2})} \qquad (5)$$

Where P is applied load, D is sphere diameter, and d is diameter of the impression left in the sample surface. Test forces range from 500 to 3000 kilograms.

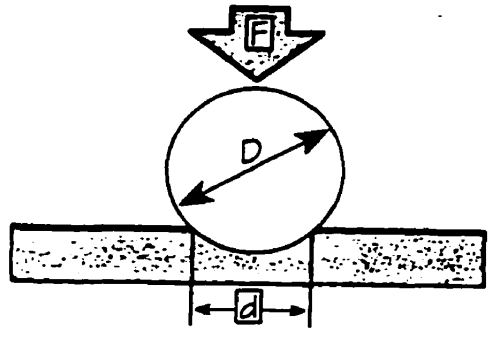

Figure (1.4.1.5.1.) Diagram Brinell Indentation (from brochure of TECH-MET CANADA LTD, JB-7/92-1M)

Vickers and Knoop Methods:

A Knoop indenter (Fig. 1.4.1.5.3) is a diamond ground to a pyramidal shape which

produces a diamond shaped indentation having an approximate ratio between its long and short diagonals of 7:1. The Vickers diamond indenter (Fig. 1.4.1.5.2) is a diamond ground in the shape of a square base pyramid with an angle of 136° degrees between faces.

To perform a test, a predetermined test force is applied with the indenter. After a specified dwell time (usually 10s), the force is removed. Then, in the Vickers method, the lengths of the vertical and horizontal axes of the indentation are measured and averaged. In the Knoop method, only the long axis is measured. The test forces range from 1 to 2000 grams (from brochure of TECH-MET CANADA LTD, JB-7/92-1M).

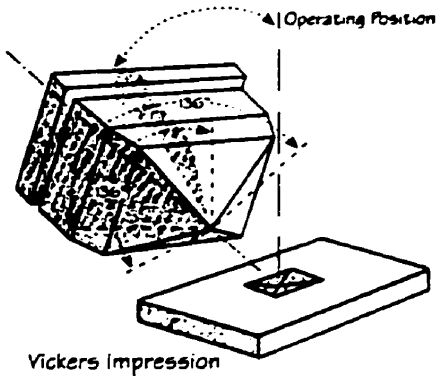

Fig (1.4.1.5.2.) Diagram of Vicker Impression •

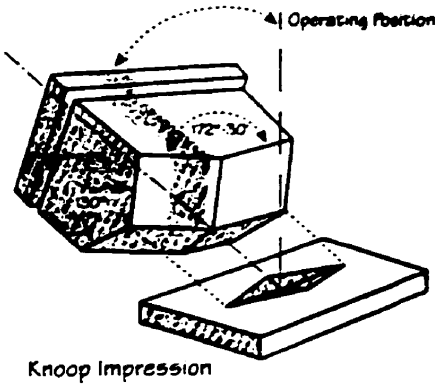

Fig (1.4.1.5.3.) Diagram of Knoop Impression•

•(from brochure of TECH-MET CANADA LTD, JB-7/92-1M)

The Knoop Hardness Number (KHN) is calculated from the projected area of the indentation.

$$KHN = \text{load / projected area} = 14.2\ P / d_2^2\ MPa \quad (6)$$

Where P is Load (N); d_2 is length of the long indentation diagonal (mm)

The Vickers Hardness Number (VHN, 136_0 Pyramid) is equal to the mean stress across

the true area of contact and is defined:

$$VHN = load / area \ \ of \ \ contact = 1.72P / d_1^2 \ \ MPa \quad (7)$$

Where P is Load (N) of contact and d_1 is the mean length of the diagonals of the indentation (mm).

ii) The Effect of Moisture on Crystal Hardness

Previous studies (Duncan-Hewitt, 1989) have investigated the effect of moisture on hardness and toughness of sucrose crystals at room temperature. The hardness of sucrose is only affected at relatively high levels of relative humidity (i.e., approximately 66%), and the toughness increases only if almost all water is excluded from the system (Duncan-Hewitt, 1988).

Water may be expected to facilitate the fracture of sucrose, just as it does that of silica (Lawn and Wilshaw, 1975). In both instances, the cohesive bonds which form the crystals are broken and these are sensitive to the presence of water which is known to decrease the apparent surface energy.

Water has been shown to act as a plasticizer which facilitates the deformation of carbohydrate polymers (Zografi, 1987). In plastics, a plasticizer penetrates between the chains to decrease their interactions and thereby decrease the yield stress.

1.4.2. Viscoelasticity in Powder Compaction

1.4.2.1 Tablet Compaction

The formation of a pharmaceutical tablet by the compression of a powdered or granular material into a cohesive mass is a complex and irreversible dynamic process. Often it is considered to occur in the following stages (Carstensen, 1980; Lieberman *et al.*, 1989; Wray, 1992):

1) Particle rearrangement (Fig 1.4.2.1 a): After the powder is delivered into the tablet die, the particles within the die flow and rearrange so that the porosity of the powder bed is decreased.

2) Elastic Deformation: After densification to a limiting closely-packed arrangement of the particles, the particles will begin to deform elastically at their points of contact (Fig 1.4.2.1a). Significant bonding does not occur at this phase.

3) Plastic Deformation: Further movement of the punch takes the applied stress beyond the elastic limit at the interparticulate contacts and permanent deformation begins. The particles may undergo plastic deformation (Fig 1.4.2.1c) or they may fracture, but in either case, the interparticulate contact areas increase and particle-particle bonds will form. Consolidation continues toward a limiting density by plastic and/or elastic deformation.

4) Ejection: After the axial pressure has been removed and the tablet is ejected, it undergoes elastic recovery (Fig 1.4.2.1c). The tablet volume increases as it is removed from the die.

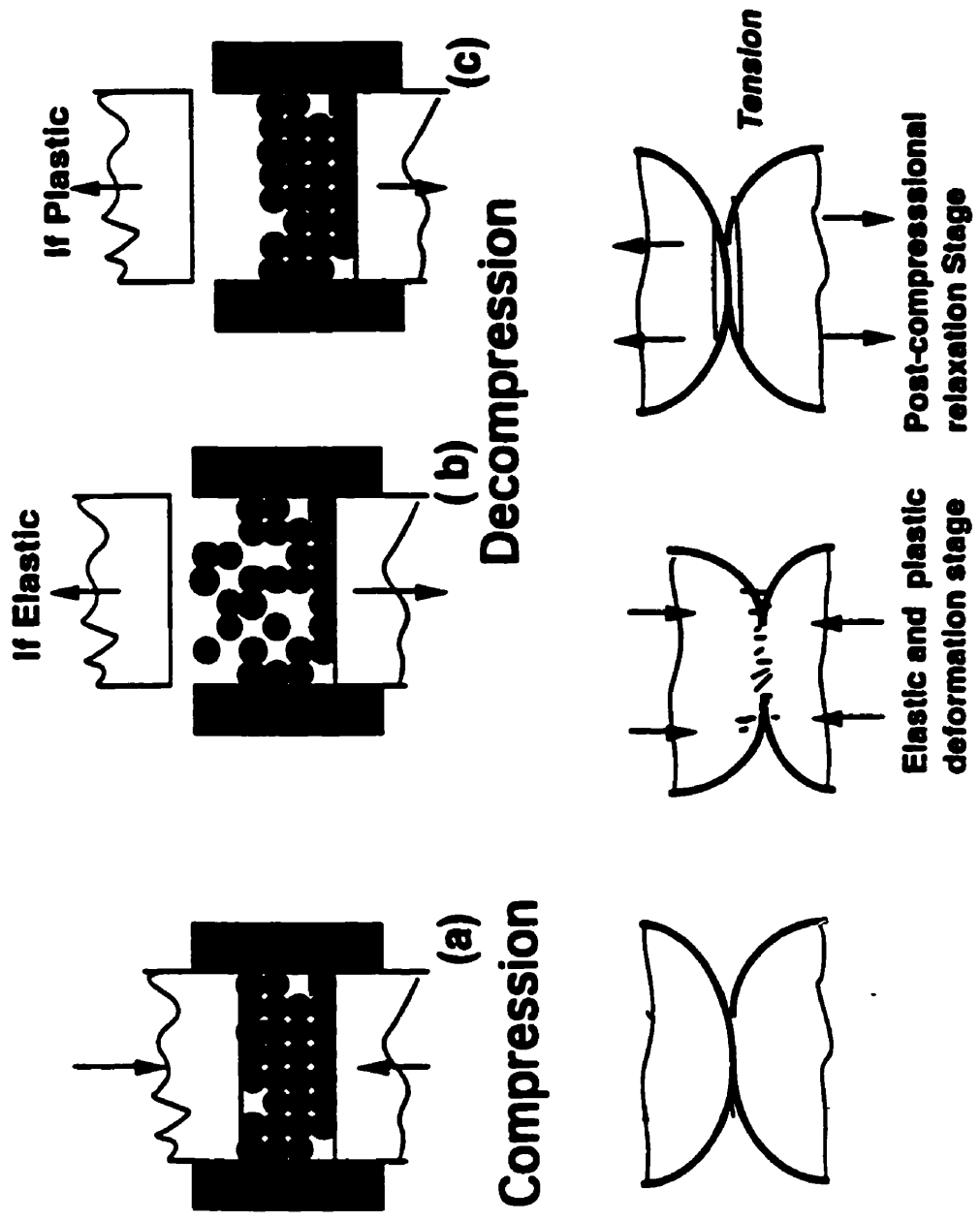

Fig 1.4.2.1.Diagram of the physical process of powder compaction

1.4.2.2. Tablet Stress Relaxation and the Viscoelastic Model of Powder Compaction

Stress Relaxation Test

Stress relaxation tests used in compression physics aim to determine the predominant mechanisms during consolidation and to correlate the characteristics thus obtained with the properties of tablets. Stress relaxation is measured just prior to the decompression stage by arresting the punch at maximum travel.

David and Augsburger (1977) modeled pharmaceutical materials as Maxwell fluids and used stress relaxation measurements to examine the time dependent behaviour of tablets. Stress relaxation data are fitted to a linearized form of the equation for a Maxwell fluid as follows:

$$\ln \sigma = \ln \sigma_{\cdot} - (\frac{E}{F})t \qquad (8)$$

where:

σ is the amount of the compressional force left in the viscoelastic region at time t, and

σ_0 is the total magnitude of this force when t=0.

The ratio (E/F), the first order rate constant which David and Augsburger termed the viscoelastic slope, was found to be larger for microcrystalline cellulose and starch than for sugar and dicalcium phosphate.

Rees and Rue (1978) performed stress relaxation experiments on a reciprocating

tablet machine and found the Maxwell model to be inadequate to characterize the stress relaxation behaviour of the materials listed above. They suggested that another model, such as that describing the behaviour of a standard linear solid (a Kelvin solid and a spring in series) might be better suited.

Bangudu and Pilpel (1984) measured the changes of tablet thickness during compression and recovery to characterize the elastic behaviour and stress relaxation behaviour and provide a correlation with tablet tensile strength. Their definitions of SR (stress relaxation) and ER (elastic recovery) are as follows:

$$SR = \left[\left(H_p - H_t \right) / H_t \right] 100\% \qquad (9)$$

$$ER = \left[\left(H_o - H_p \right) / H_p \right] 100\% \qquad (10)$$

Where:

H_O is the thickness of the tablets when first formed, H_p and H_t are the thicknesses of the tablet at the maximum pressure and after being held for 30 seconds at the maximum pressure, respectively.

Although this method has the advantage of simplicity and ease of operation, the parameter values derived from it may vary with different test conditions so their predictions may not be consistent because factors such as die wall friction, anelasticity, fracture, porosity and the time dependence of tablet compaction were not considered.

Viscoelastic Model

Rippie and Danielson (1981) used a three-dimensional viscoelastic model to describe

tablet behaviour during the unloading portion of the compression event. For a three dimensional situation the state of stress in a tablet must be expressed by tensor (*s*) of the form:

$$S = \begin{vmatrix} s_{xx} & s_{xy} & s_{xz} \\ s_{yx} & s_{yy} & s_{yz} \\ s_{zx} & s_{zy} & s_{zz} \end{vmatrix} \qquad (11)$$

where s_{ZZ} is the axial (punch) stress, s_{XX} and s_{YY} are the radial (die) stresses and the other quantities are the shear stresses. The nine stress components are illustrated in Fig 1.4.2.2.1.

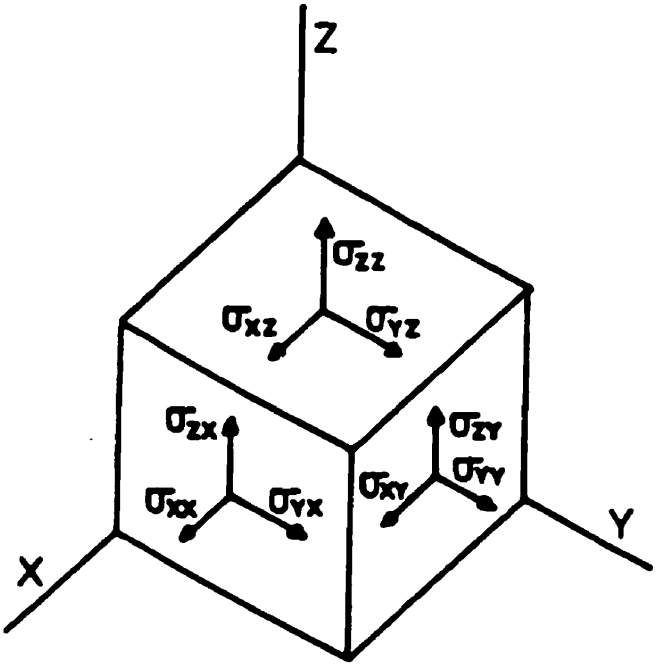

Fig 1.4.2.2.1 Stress components acting on a cubical element within a stressed body (Rippie and Danielson, 1981)

The three-dimensional viscoelastic theory, used in the data analysis, provides for the separate characterization of tablet behaviour into its dilation and distortion components. The tablets investigated were found to behave elastically in dilation, but to have both viscous and elastic contributions to their stress/strain relaxation in distortion. A dependence of the viscous and elastic parameters on the compression conditions was found to be predictive of conditions under which capping or lamination of the compact would occur.

Casahoursat and coworkers (1988) used a more complex viscoelastic model to describe stress relaxation. Their bi-or tri-exponential equation for stress decay is analogous to two or three Kelvin solids and an individual spring in series or the same number of Maxwell elements and an individual spring in parallel.

Although linear viscoelastic theory has been applied to the analysis of stress relaxation behavior, these models do not adequately fit the experimental data (Rippie and Danielson, 1981; Duncan-Hewitt, 1989) and have limited success at predicting the performance of tablets (Rippie and Danielson, 1981; Casahoursat *et al.*, 1988).

Because linear viscoelasticity theory is unsatisfactory to characterize post consolidation (*i.e.* stress relaxation) of most materials, Papadimitropoulos and Duncan-Hewitt (1992) analyzed the stress relaxation of sodium chloride and potassium bromide tablets using a model of interparticulate contact stress relaxation based on the non-linear deformation kinetic theory. Furthermore, Lin (1992) extended the use of this model to investigate the stress relaxation of acetaminophen. They found that the stress relaxation data for this material fitted the proposed model and yielded activation parameters which could eventually play a critical role in the prediction of capping.

1.4.2.3. Deformation Kinetics Theory

The microscopic physical process that underlies plastic deformation and crack growth is the breaking of atomic bonds at high energy sites. In plastic flow, the bonds between the atoms of the solid are broken, rearranged, then reformed. In crack growth, bonds are broken at each step but no new bonds are formed (Krausz and Krausz, 1988). Thus all plastic deformation processes are composed of the elementary steps and their characteristic rates of breaking and re-forming of atomic bonds. The combination of these steps and their characteristic rates control the character of all deformation mechanisms. The thermally activated plastic deformation process therefore can be compared with chemical reactions, and the analysis of plastic flow may be carried out by using the methods of chemical kinetics (Hanley and Krausz, 1974.; Krausz and Krausz, 1988).

During plastic deformation, a dislocation is stopped in front of an obstacle which acts as an energy barrier to further flow. It remains there until the combined effect of the stress and thermal energy increases the energy of the atoms sufficiently to overcome the barrier. The energy barriers (Fig.1.4.2.3.1) may form either a parallel system, a consecutive system, or a combination of these two types (Krausz and Eyring, 1975).

For a system of m parallel barriers the kinetic equation can be expressed as (Krausz and Eyring, 1971):

$$\dot{\gamma} = \sum_{j=1}^{m} \delta_j (\rho_{fj} k_{fj} - \rho_{bj} k_{bj}) \qquad (12)$$

where δ is the contribution to the deformation rate by each activation, the subscripts f and b indicate that the activation is associated with the forward or backward flow over the

jth barrier, respectively, and ρ is the concentration of flow units (mobile dislocation density or vacancy concentration). k_j is the rate constant of the jth-type energy barrier.

For n consecutive barriers then, the deformation rate is (Krausz and Eyring, 1971):

$$\frac{1}{\dot{\gamma}} = \frac{1}{\delta}\left(\sum_{j=1}^{n} t_j\right)\left[\rho_1 - \rho_{n+1} t_{n+1}^{-1} \upsilon^{-1}\right]^{-1} \qquad (13)$$

where tj is the relaxation time ($tj=1/k_j$), and υ the pre-exponential frequency factor $K\frac{kT}{h}$. k is Boltzman's constant and K is the transmission coefficient.

The rate of each step is defined by the appropriate rate constant according to the absolute rate theory as (Hanley and Krausz, 1974):

$$k_j = K_j \frac{kT}{h}\frac{F_j'}{F_j}\exp\left(-\frac{\Delta E_i \pm V_i \tau}{kT}\right)$$
$$= A_j \exp\left(-\frac{\Delta E_i \pm V_i \tau}{kT}\right) \qquad (14)$$

where K is the transmission coefficient, F_j' and F_j are the partition functions associated and reactant states, respectively, ΔE_i is the activation energy, V is the activation volume, the $\pm$ sign indicates whether the process is associated with forward (-) or backward (+) activation, A_j is the pre-exponential factor, and τ is shear stress.

i) Explicit Equations for One Energy Barrier to Deformation

The simplest means to illustrate plastic deformation as a chemical process is the situation which arises when only one mechanism that is symmetrical at equilibrium, with a

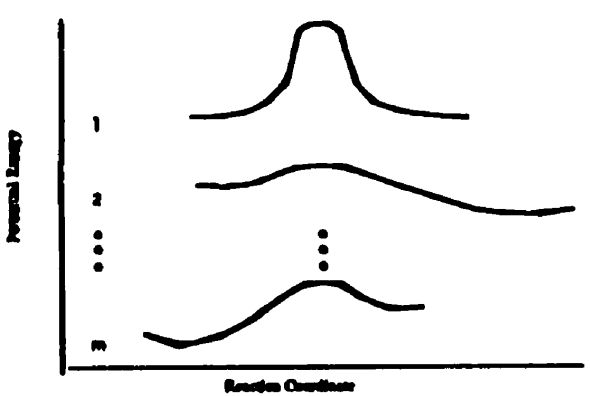

a parallel system

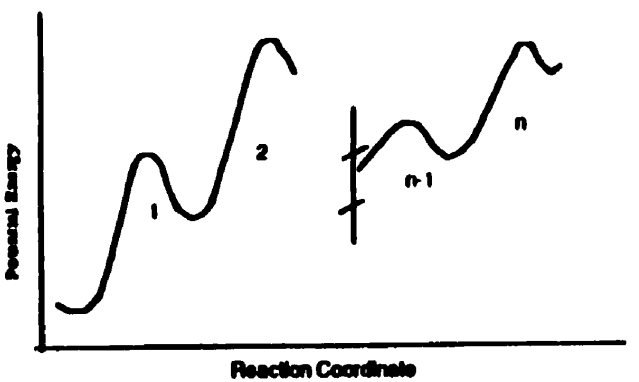

a consecutive system

Fig.1.4.2.3.1. Schematic of energy barriers for a parallel system and a consecutive system (Krausz and Eyring, 1975)

single-energy barrier, controls the rate of deformation (Krausz and Eyring, 1975).

At high stress, the deformation rate is controlled only by activation in the forward direction over a single energy barrier (Krausz and Eyring, 1975) i.e., backward flow is assumed to be negligible. The kinetic equation can be expressed as:

$$\dot{\gamma} = \delta_1 \rho_{f1} k_{f1} \tag{15}$$

Substituting Eq.14 into Eq.15, the experimental data are often expressed by the Arrhenius equation as:

$$\begin{aligned} \dot{\gamma} &= \delta_{f1} \rho_{f1} K_{,} \frac{kT}{h} \frac{F_{,}}{F_{,}} \exp[-(\Delta E \pm V\tau)/kT] \\ &= \nu_e \exp[-(\Delta E \pm V\tau)/kT] \end{aligned} \tag{16}$$

Where: ν_e is the pre-exponential frequency factor

or

$$\ln \dot{\gamma} = \ln(\delta \rho_1 A_1) + V_{f1} \tau / kT \tag{17}$$

Because the deformation rate is controlled by activation in the forward direction, Eq.(16) can be expressed as:

$$\dot{\gamma} = \nu_e \exp[-(\Delta E - V\tau)/kT] \tag{18}$$

At a high enough stress and over the initial period of relaxation, the stress relaxation behavior of most materials is usually logarithmic, that is it adheres to a linear dependence of

log $(-\dot{\gamma})$ on τ which corresponds to flow in the forward direction over a single energy barrier. At lower stresses the behavior becomes noticeably nonlinear and a more complex kinetic equation must be considered. The next level of complexity takes into account the backward movement of the flow units over the energy barrier. The kinetic equation then is (Hanley and Krausz, 1974):

$$\dot{\gamma} = \delta_1(\rho_{f1}k_{f1} - \rho_{b1}k_{b1}) \qquad (19)$$

The first term in Eq 19 can be evaluated over a high stress range. The second term can be determined by rearranging Eq 19 and introducing Eq.14 in the following form:

$$\ln(\delta_1\rho_{f1}k_{f1} - \dot{\gamma}) = \ln \delta_1\rho_{b1}k_{b1} = \ln(\delta\rho_{b1}A_1) - V_{b1}\tau / KT \qquad (20)$$

$\ln(\delta_1\rho_{f1}k_{f1} - \dot{\gamma})$ is plotted versus τ. From the slope and intercept of the resultant straight line, the backward activation volume and the pre-exponential factor can be determined.

ii) Explicit Equations for Two Energy Barriers

In plastic deformation, it is also necessary to consider that the relaxation may occur over a system of energy barriers before any final appreciable contribution is made to the flow. One of the simplest systems consists of two consecutive flow units.

When two energy barriers are connected in series, the rearrangement of Eq. (13) leads to (Hanley and Krausz, 1974):

$$\ln[\frac{\delta\rho_1}{\dot{\gamma}_1}(1-\frac{\rho_3}{\rho_1 v t_3})-1]=\ln(\frac{A_1}{A_2})-\frac{V_{b1}+V_{f2}}{2kT}\sigma_a \qquad (21)$$

Because t_3 represents the relaxation time in the backward direction over the whole barrier system and $\frac{\rho_3}{\rho_1 v t_3}$, associated with the backflow, is much smaller than unity, it can be neglected at this stage. An analysis was carried out with Eq. (21) and this equation was written in the following form for the first step of the second-barrier analysis:

$$\ln(\frac{\delta\rho_1\kappa_1}{\dot{\gamma}}-1)=\ln(\frac{A_1}{A_2})-\frac{V_{b1}+V_{f2}}{2kT}\sigma_a \qquad (22)$$

In Eq.(22) the term $\delta\rho_1\kappa_1$ can be determined from the single-barrier analysis (Eq.17; Eq.15.) and the term log $(\frac{\delta\rho_1\kappa_1}{\dot{\gamma}}-1)$ can be plotted as a function of the measured stress. Therefore, the composite activation volume of $V_{b1}+V_{f2}$ can be evaluated from the slope.

iii) Estimation of Activation Energy and Activation Volume.

The activation energy (the height of the barrier) and activation volume (the extent of the barrier to deformation) are two fundamental parameters associated with each barrier to deformation, the mathematical description of which will be discussed in this section.

The Experimental Activation Energy

Although the strain rate can not be measured in a stress relaxation experiment, the shear stress rate can be calculated if stress is measured as a function of time, and the relationship between shear stress rate ($\dot{\gamma}$) and strain rate ($\dot{\tau}$) is known by using the Halsey-Eyring 3-

element model (consisting of a spring, and a Maxwell unit including a linear spring and a non-linear dashpot) (Fig.1.4.1.3.2.). In stress relaxation, the strain rate of the non-linear Maxwell element of the 3-element model must satisfy the condition that the total strain rate is equal to 0. Using the following relationship between shear stress rate ($\dot{\tau}$) and strain rate ($\dot{\epsilon}$), one obtains (Papadimitropoulos, 1990):

$$\dot{\gamma}_{total} = \dot{\gamma}_{el} + \dot{\gamma}_{visco} \tag{23}$$

$$\dot{\gamma}_{visco} = -\dot{\gamma}_{el} = -\frac{\dot{\tau}}{E} \tag{24}$$

$$\dot{\tau} = -E\dot{\gamma}_{visco} \tag{25}$$

where: E is the elastic modulus.

Substituting Eq. 25 into 18:

$$\dot{\tau} = -Ev_e \exp[-(\Delta E - V\tau)/kT] \tag{26}$$

or

$$\ln \dot{\tau} = -\ln Ev_e - \Delta E/kT + V\tau/kT \tag{27}$$

It can be shown from Eq.(27) that the experimental apparent activation energy can be expressed as:

$$\Delta E = -k\frac{\partial \ln \dot{\tau}}{\partial(1/T)} \tag{28}$$

The activation energy can be evaluated using the slope of plot of ln (shear stress rate)

versus the inverse absolute temperature at constant stress.

The Experimental Activation Volume

The activation volume is a characteristic quantity of plastic flow, and it has an important role in the analysis of the rate controlling process as has the activation energy. As a rule, in calculations for crystalline materials (Hirth and Lothe, 1968; Nabarro, 1967), the length of the dislocation segment multiplied by the stress is considered to be equal to the force that does the work, and the distance over which the work is done is related to the activation path or to the size of the obstacle. Activation volume can then be defined as follows:

$$V = kT \frac{\partial \ln(d\dot{\tau})}{\partial(\tau)} \qquad (29)$$

The activation volume can be calculated from a plot of ln (shear stress rate) versus the average shear stress at constant temperature.

Table (1.4.2.3.3) shows typical ranges of activation volumes for some deformation mechanisms. These volume are usually related to the Burgers vector (b) (the shortest distance a dislocation can travel).

Table 1.4.2.3.3. Deformation Mechanisms and their Associated Activation Volumes (Krausz and Eyring, 1975)

Mechanism	Vact
Climb Mechanism	1 b^3
Peierls-Nabarro mechanism	$10\text{-}10^2$ b^3
Intersection Mechanism	$10^2\text{-}10^4$ b^3

1.4.2.4. Interparticule Bonding in Tablets

The successful formation of a pharmaceutical tablet by the compression of solid particulate matter depends on bonding across particle-particle interfaces which are formed during compression. However, decompression and ejection may cause these bonds to break (Danielson *et al.*, 1983). Mechanical theory, intermolecular theory, and liquid surface film theory are three major approaches that have been used to explain bonding in the compression process (Lieberman, *et al.*, 1989).

The mechanical theory proposes that under pressure the individual particles undergo elastic, plastic, or brittle deformation and that the edges of the particles intermesh, forming a mechanical bond. Mechanical innterlocking is not a major mechanism of bonding in tablets.

The intermolecular force theory is that, under compressional force, the molecules (or atoms or ions) at the points of contact between newly formed surfaces of the granules are close enough so that van der Waals' forces are significant.

The liquid-surface film theory attributes bonding to the presence at the particle interfaces of a thin liquid film, which may be the consequence of fusion or adsorbed moisture. For materials that may be compressed directly, the liquid surface film theory proposes that the liquid film is a result of fusion or solution at the surface of the particle induced by the energy of compression. During compression, the force is applied to a small area of true contact so that a very high pressure exists at the true contact surface. The local effect of the high pressure on the melting point and solubility of a material is essentially bonding. The evidence that was used to support this theory is that granulations that are absolutely dry have poor compressional characteristics (Train and Lewis, 1962).

Water or saturated solutions of the material being compressed may form a film that acts as a lubricant, and if less force is lost to overcome friction, more force is utilized in compression and bonding, and the ejection force is reduced. In formulations using solutions of hydrophilic granulation agents, there may be an optimum moisture content. It has been reported that the optimum moisture content for the starch granulation of lactose is approximately 12% and phenacetin is approximately 3% (Sheth and Munzel, 1959).

Hiestand (1991a) modeled the processes involved in tablet bonding by considering the effect that the viscoelastic properties of the material have on the strength of bonding. At lower compression forces compaction may be the result of ductile processes, but at higher compression forces a brittle compaction mechanism may occur. The bond force between two identical viscoelastic particles where ductile deformation does not occur was described using the following equation:

$$f_a' = -\frac{2\varepsilon_t H_0 \Delta\tau}{\varepsilon_- \varepsilon_0 H_c}\left(\frac{f_c}{\pi H_c}\right)^{\frac{1}{2}} \qquad (30)$$

whereas the bond strength in the presence of ductility was described by:

$$f_{ad} = -H_t \pi a_d^2 = -\left(\frac{64}{\pi H_t^3}\right)\left(\frac{H_o \Delta\tau}{\varepsilon_o}\right) \qquad (31)$$

Where:

a_d: maximum chordal radius of contact for ductile extension;

f_a': pull off force; spherical surfaces; brittle mechanism; viscoelastic material;

f_{ad}: pull off force;spherical surfaces, ductile extension of surfaces;

f_c: compression force; spherical surfaces;

H_0: indentation hardness for instantaneous process;

H_t: indentation hardness for viscoelastic materials where strain rate is based on the process rate using time t;

H_c: indentation hardness of particles at strain rate used for the compression of the compact;

$\Delta\gamma$: change of surface energy going from free surface to solid interface;

ε_0 ε_T ε_-: strain indices.

In addition, Heistand indicated that materials undergoing ductile extension must not only satisfy the condition that compression force is (f_c) very low (Eq.32), but also should be meet the condition that the R be smaller than a critical value (Eq. 33).

$$f_c < \left(\frac{256\, H_c}{\pi}\right)\left(\frac{\varepsilon_- H_o \Delta\tau}{\varepsilon_T \varepsilon_o H_t^2}\right)^2 \qquad (32)$$

$$R < \frac{64\, H_0 \Delta\tau}{\pi^2 \varepsilon_T \varepsilon_o H_t^2} \qquad (33)$$

where: R is the harmonic mean radius of the two contacting spherical surfaces.

This bonding theory was examined experimentally (Hiestand, 1991b). It was found that sorbitol underwent a ductile to brittle mechanism transition with increasing compression forces, while phenacetin illustrates one brittle mechanism in the whole process.

30

1.4.2.5. Mechanical Strength of Tablets

A tablet requires a certain amount of strength, or hardness, to withstand mechanical shocks when handled, and subsequent other process. Moreover, a tablet hardness may also influence the tablet disintegration and drug dissolution rate (Lieberman, *et al.*, 1989 Vol 2.). The term of *mechanical strength* has been used sometimes quite ambiguously in reference to tablets. It is sometimes termed tablet *crushing strength*, *friability*, and *hardness*.

Tablet Strength Testing

The tensile strength (S_E) of a tablet quantifies its resistance to fracture. The crushing strength is the parameter most widely measured, and is defined as the force required to break a tablet in a diametral compression test. Generally the process can be described as that if a knife-edged anvil is used or the anvil and plunger faces coming into contact with the tablet are padded, the specimen may fail in tension and therefore the strength s_E can be calculated from (Fell and Newton, 1968):

$$\sigma_E = \frac{2F}{\pi DL} \qquad (34)$$

Where F is crushing force applied to the tablet, D is the diameter of the tablet, and L is tablet thickness.

In 1977, Hiestand *et al.* proposed a technique for assessing the elastic-plastic behaviour of a material by comparing the strength of a tablet that contains a central axial hole with one that does not. If the tensile strength of tablet without the hole is T_S and that of the tablet with the hole is T_O, Hiestand defined the Brittle Fracture Index, BFI, as

$$BFI = \frac{(T_s - T_o)}{2T_s} \qquad (35)$$

Residual stresses are concentrated around the hole and reduce the tensile strength of the annular tablet, so the difference between the two tablets is claimed to give a measure of the stress relief that results from plastic flow during compression. Low values for the BFI show plastic behaviour, high values show elastic behaviour.

Tensile strength measurements on tablets are usually indirectly derived from diametrial compression or one of the flexure tests. Nyström *et al.* 1978 used a direct method, in which the specimen is held at each end and is pulled apart, in a series of tests on aspirin and paracetamol tablets with varying amounts of polyvinylpyrrolidone (PVP). Nyström *et al.*, 1978 compared these axial tensile strengths as determined on a Heberlein (Schleuniger 2E/205) tester, and found that the addition of PVP increased the axial strength without affecting the radial strength to any great extent. This change in the relative strengths resulted in a decreased capping tendency.

Various attempts have been made to combine *hardness* and *strength* into a

meaningful equation that would be of value to the formulator, and some of this work is discussed in a paper by Jetzer (1986). It is suggested that useful information can be obtained by comparing the two types of hardness measurement, and that this may help in the prediction of capping tendencies.

Friability

The friability of a tablet is related to its hardness, but is more directly a measure of its resistance to chipping and abrasion during storage and transport. The test for that property is almost universally carried out on an instrument which consists of a rotating drum with internal baffles. Tablets in the drum are lifted and dropped by these baffles throughout the test period, and their resultant loss in weight is taken as a measure of their friability. A modification of the friability test has been proposed by Duncan-Hewitt and Grant (1987), and is described as the impact fracture wear test. For this test, the tablets are placed in a sieve, which is vibrated mechanically in a horizontal plane by means of a 'Vortex Genie' drive motor until the sample has lost at least 50% of its original weight.

1.4.2.6. *Effect of Moisture on the Mechanical Behaviour of Tablets*

The presence of moisture in pharmaceutical powders can have a significant impact on their flow and compression characteristics by affecting the interparticle bonding properties. The crystallization of dissolved material can lead to the formation of solid bridges between particles due to the movement of water within the tablet (Rees and Hersey, 1972; Hall and Rose, 1978; Ahlneck and Alderborn, 1989b). In addition, adsorbed moisture is important particularly with respect to the physical and chemical

stability of drugs (York, 1983; Alderborn and Ahlneck, 1991).

Moisture can be present in powders in different physical forms: as an adsorbed monolayer or multilayers on the particle surfaces, as condensed water on the surface, as physically absorbed water within the particles, or as strongly bound chemisorbed water. The presence and distribution of moisture in the above forms will depend considerably on the chemical nature of the particulate material, its physical properties (such as particle size and porosity), and on the ambient relative humidity which determines the equilibrium moisture content (the amount of moisture in a solid for a given temperature and moisture level in the surrounding air) (York, 1981; Khan and Pilpel, 1987; Malamataris *et al.*, 1991).

The analysis of sorption isotherms of excipient can differentiate "bound" ("solidlike") and "free" water (Zogrfai and Kontny, 1986). It has been observed that the removal of unbound water reduces the ability of microcrystalline cellulose (Hüttenrauch, 1977) and compressible sugar (Zografi and Kontny, 1986) to act as direct-compaction materials. This is because that free water is needed to provide plasticity to these systems. Free water on the external surface of powders can also affect powder flow (Armstrong, 1970).

i) Thermodynamic and Kinetic Aspects of Moisture Sorption

Water can associate with solids in two ways. Water molecules can interact only with the surface of the solid (adsorption) or penetrate the bulk solid structure (absorption). When both adsorption and absorption occur, the term 'sorption' often is used.

Edgar and Swan (1922) presented one of the first studies of the thermodynamics and kinetics of moisture sorption and predicted that the rate of moisture adsorption could be expected to depend on: (1) the difference between the partial pressure of water vapour in the atmosphere and that above the saturated aqueous solution of the hygroscopic substance; (2) the temperature; (3) the surface area of the solid exposed to water vapour; (4) the "velocity of movement" of the moist air, and (5) a "reaction constant" characteristic of the solid.

Markowitz and Boryta (1961) defended the theoretical suitability and experimental advantage of the thermodynamic approach. They chose the negative value of the free energy change accompanying the transfer of water to the condensed (absorbed) phase from the atmosphere, as driven by the imbalance of chemical potential of water between the two systems as a criterion for hygroscopicity. They named the $-\Delta G$ value the "hygroscopicity potential" (HP) as given by:

$$HP = -\Delta G = \mu_{H_2O.pure} - \mu_{H_2O.sys} = RT\ln[\frac{P_{H_2O.pure}}{P_{H_2O.sys}}]. \qquad (36)$$

Because such thermodynamic measurements are unable to resolve the individual factors upon which this rate depends, it is of little theoretical significance.

Zografi and his coworkers (Van Campen *et al.*, 1980. Van Campen *et al.*, 1983a. and b. Kontny, *et al.*, 1987) designed specialized equipment for more precise determination of the rate and extent of moisture sorption. They developed a model based on the fact that the heat of condensation of water released during water uptake must be transported to the surroundings. In an atmosphere of pure water vapour, where diffusion does not occur, this heat flux limits the rate of condensation. The equation they developed to

determine the water uptake rate is as follows:

$$W_h' = (C+F)\ln(\frac{RH_i}{RH_o}) \qquad (37)$$

Where the water uptake rate, W_h', is constant at a given relative humidity, C and F are conductive and radiation coefficients, RH_i is the relative humidity and RH_o is the critical relative humidity of a substance associated with the relative humidity in equilibrium over a saturated solution of the substance.

The critical relative humidity (RH_o) which exists over a saturated solution of the material determines the minimum RH at which adsorption will proceed to any significant extent (Van Campen *et al* 1987). Above its RH_o, the material will adsorb water until the adsorbed film is sufficiently diluted for its vapour pressure to be in equilibrium with the atmosphere. Solids deliquesce or dissolve in the adsorbed layer of water. For a highly soluble compound this readily leads to complete dissolution or deliquescence, at a rate governed by the difference, RH_S (i.e., RH_i-RH_o) and by sample size. Once deliquescence has occurred, further moisture uptake depends on the solution properties of the dissolved substance.

Below RH_o, there exists no driving force sufficient to cause further adsorption. Dissolution of a crystalline solid into adsorbed water (surface dissolution) would not be expected to occur below RH_o. At most 2-3 layers of vapour can be adsorbed onto the clean, dry surface of a substance associated with the equilibrium water vapour pressure over a saturated solution of the solid (Walter, 1971; Kaiho *et al.*, 1972; Barraclough and Hall, 1974; Chikazawa and Kanazawa, 1978). However, Kontny *et al.*, (1987) recently showed that mechanical processes of solids such as grinding, milling, micronization, compaction, etc., can induce changes in the reactivity of a material toward water vapour.

As a result, the surface dissolution of drug may occur at a lower humidity, which may lead to chemical and physical instability problems during subsequent storage.

For soluble drug substances, the amount of water needed to reach RH_0 is quite small (i.e., the relative humidity over the saturated solution is low). Conversely, for poorly soluble materials it is quite high (Cartensen and Li, 1992).

ii) The Effect of Moisture on Crystal Strength

There is evidence to suggest that moisture can markedly affect mechanical strength and may even minimize some failure that occurs during compression. Chowhan and Palagy (1978), found that partial moisture loss from stored tablets induced an increase in tablet strength, possibly through recrystallization of soluble excipients within voids. Later work by Chowhan (1980) indicated that the increase in strength was linearly related to the amount of moisture lost after compression, but that the disintegration time was not affected.

In 1981, Khan *et al.*, examined the influence of the moisture content of microcrystalline cellulose on the compressional properties of some formulations and found that a decrease in moisture content reduced its compressibility. It was suggested that the presence of an optimum amount of moisture would prevent elastic recovery by lowering the yield point and promoting the formation of bonds through hydrogen bridges.

Pilpel and Ingham (1988) studied the effect of moisture on the density, compaction and tensile strength of microcrystalline cellulose. They related the changes in mechanical properties of the material and the tensile strength of its compacts to the way in which water is sorbed into the cellulose structure. The yield pressure (the inverse slope of the

Heckel plot) was observed to decrease with increasing water content. The effect was attributed to disruption caused by the water on the hydrogen bonds cross-linking the cellulose hydroxyls causing the cellulose to become plasticized.

Li and Peck (1990) studied the effect of moisture on the compression properties of maltodextrin powders. An increase in the moisture content of the powder reduced the yield pressure and improved the densification for all five maltodextrins evaluated. Compacts produced by maltodextrins with a lower degree of polymerization exhibited a greater tensile strength for a given pressure at a moisture content below 8.0%. A further increase in moisture content resulted in a decrease in compact tensile strength.

In 1991, Shukla and Price reported that an increase in the moisture content of lactose resulted in a reduction in strength of the tablets which could be attributed to a decreased binding strength between the particles. Moreover, increased water content gave rise to increased pressure requirements to achieve specified hardness values. In tests of sucrose and sodium chloride, Alderborn and Ahlneck (1991) demonstrated that the strength of a tablet exposed to humid air can change markedly during storage. Malamataris *et al.* (1991) reported the relationship between moisture sorption and the tensile strength of some direct compression excipients. Tensile strength was observed to reach a maximum value and then decrease when the moisture content was about double that corresponding to a tightly bound monomolecular layer. The changes in the mechanical characteristics were explained by the combined effect of moisture on interparticle and intermolecular forces.

Garr and Rubinstein (1992) studied the influence of moisture content on the consolidation and compaction properties of paracetamol. The mean yield pressure (the inverse slope of the Heckel plot) was observed to decrease with increasing moisture

content which they attributed to the overall plasticizing effect of moisture, while relative powder density increased which was hypothesized to be due to lubrication effects.

The above results suggest that the hardness and strength follow a general pattern (Armstrong and Patel, 1986; Li and Peck, 1990; Malamataris *et al.*, 1991; Alderborn and Ahlneck, 1991) with increasing moisture content, that is, an initial increase in tablet strength followed by a reduction.

It may be that initially tablet strength increases indirectly due to the lubrication effect of water which improves force transmission from the upper to lower punch, facilitating greater powder consolidation, and which facilitates the formation of the interparticle hydrogen bonding (Zografi and Kontny, 1986; Li and Peck, 1990; Malamataris and Dimitrious, 1991; Garr and Rubinstein, 1992). Alternatively, it may increase the interparticle van der Waals' forces by smoothing the surface microirregularities and reducing the interparticle separation (Eaves and Jones, 1972). The subsequent decrease in hardness and strength with higher moisture content may be attributed to water forming surface films on the particles which act as a physical barriers for interparticulate bonding (Ree and Hersey, 1972). The presence of less tightly bound 'absorbed' or 'bulk' water increases the plasticity and weakens the interparticle bonds (Malamataris and Dimitrious, 1991).

1.4.3. Investigation of Capping/Lamination and Proprosed Solutions

1.4.3.1. *Investigation of Some Failure Mechanisms*

Powder technology is of great interest to the pharmaceutical industry for a variety of reasons. One of most important reasons is to solve capping and lamination. Most scientists believe that the causes of capping and lamination are excessive elastic recovery and inadequate interpaticule adhesion during the post-consolidation stage (Lieberman , 1989). The excessive elastic energy is not uniformly distributed in the tablet. As discussed before, if the elastic stress exceeds the ideal fracture stress (strength of bonds) the crack will start. The Griffith Crack Theory indicates that a crack will propagate when the elastic energy at the tip of a crack is equal to the surface energy needed to form the new surfaces.

1.4.3.2. *Approaches to Solve Capping or Lamination by Optimizing Tablet Moisture Content*

As discussed previously, successful tableting also depends on the ability of the bonds within the tablet to withstand elastic recovery during decompression. Parmentier *et al.* (1980) commented that capping was associated with an inhomogeneous density distribution, coupled with low binding forces in the capping zone. The ability to bond and form solid bridges between particles is mediated or facilitated by the presence of adsorbed water. Experience has shown that capping occurs more frequently when particles are dried excessively. It was suggested that the moisture content of the material should be carefully maintained at a level where binding is optimized. While too much

moisture, could produce merely a lubricant effect, not enough moisture could lead to a weaker compact. However, the problem is avoided when suitable moisture levels are maintained with granulation (Wong and Mitchell, 1992). Moreover, the capping pressure of paracetamol compacts has been shown to increase with moisture contents up to 6% w/w and then to decrease beyond 8% w/w moisture content. So paracetamol compacts with up to 6% w/w moisture content were found to have a higher capping pressure (Garr and Rubinstein, 1992).

From a theoretical consideration of this point, both the excessive elastic recovery and inadequate interparticle adhesion contribute to capping or lamination. While moisture can not only greatly enhance the plastic deformation of the powder under compression (Li and Peck, 1990) and subsequently reduce elastic recovery, but it also may also assist in the formation of stronger bonds through hydrogen bonding.

On both theoretical and experimental grounds, moisture levels appear to play a significant role in minimizing capping or lamination occurring during compression. It would be very useful to elucidate and quantify the relevant parameters which could then be used to predict or minimize these problems.

WORKING MODEL DEVELOPMENT

2.1. BACKGROUND AND THEORIES APPLICABLE TO THE WORKING MODEL

Stress relaxation theory, viscoelastic theory, deformation kinetic theory and moisture sorption theory are employed to form the theoretical basis of this project. The rationale for the application of these theories have been or will be discussed (Fig 2.1.0.1).

2.1.1. The Assumptions that Permit the Use of This Model

The model used in this thesis is based on following assumptions:

1. Deformation kinetic theory can be used to describe the behavior of pharmaceutical materials in the presence of water.
2. Stress relaxation experiments can be used to assess activation parameters.
3. The interparticle contact area remains constant during stress relaxation.
4. The assembly of crystals, contacting each other at their aspirities, resemble the configuration of the hardness test.
5. The yield behavior, or hardness is assumed independent of the strain history.
6. The particles in a compact do not move relative to one another during stress relaxation.

2.1.2. Application of the Stress Relaxation Test to this Model

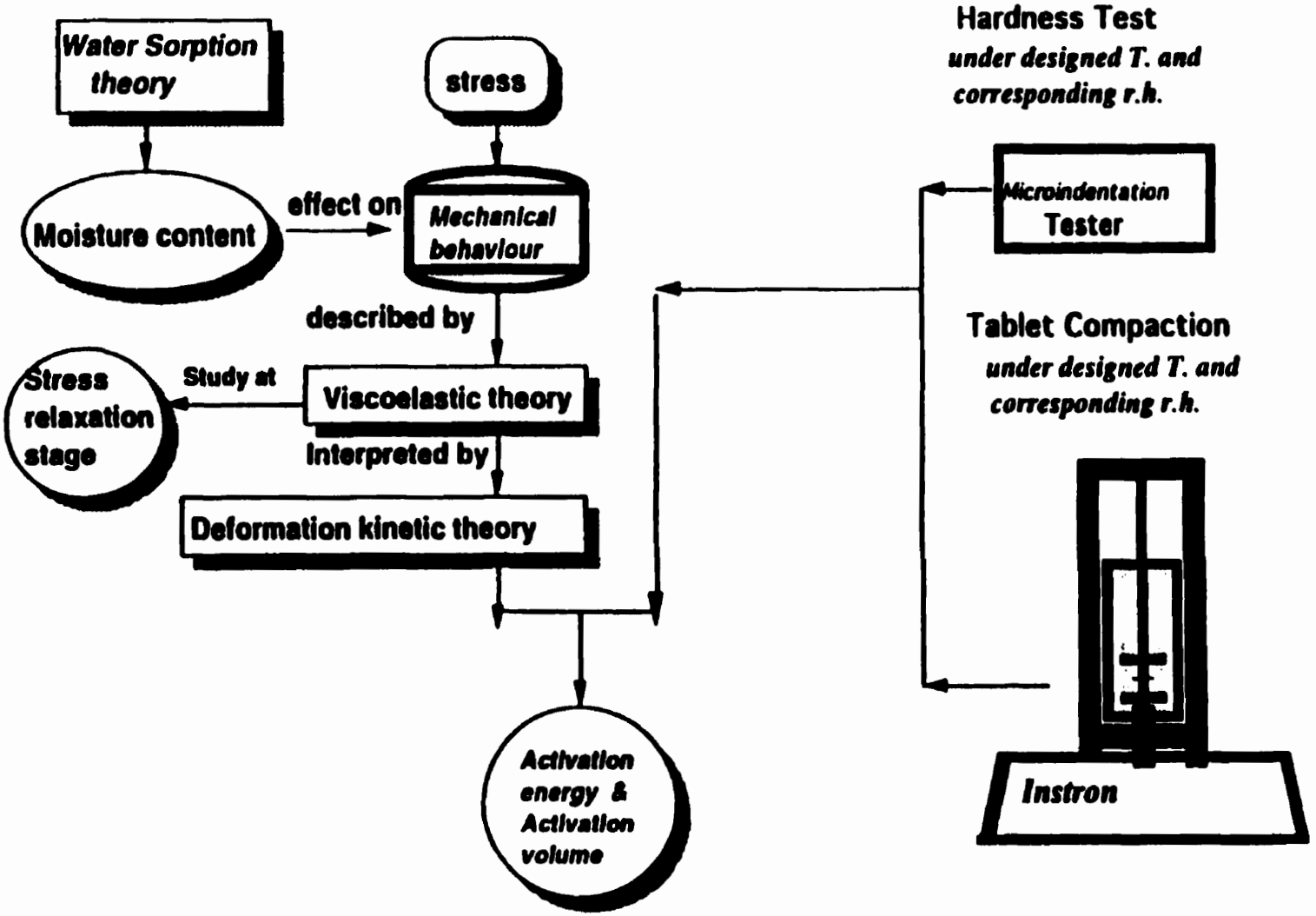

Fig 2.2.0.1. Outline of Study Design

2.1.2. Application of the Stress Relaxation Test to this Model

Stress relaxation offers a unique advantage in the study of the time dependent deformation of crystalline materials since very little plastic deformation takes place during the measurement period which helps minimize complications due to fracture. Another significant advantage of the stress relaxation test is that a wide range of strain rates and stresses can be evaluated in a single experiment. Stress relaxation was considered to be an appropriate technique to use in the characterization of the kinetic characteristics of pharmaceutical materials because capping and lamination occur during the post-compressional relaxation stage of tablet compaction. Technically, the stress relaxation measurement is complicated by the fact that it is necessary to measure relaxation over the very short initial time period to determine mechanisms that may be operative during tablet compaction (which usually is very rapid).

As discussed above, the deformation of sucrose is expected to arise from several mechanisms -- those inherent to the material itself at zero moisture levels, and also those associated with its interaction with water at higher levels of relative humidity. It is expected that if different mechanisms control the rate of deformation at different levels of moisture content, this will be apparent in changes in activation parameters as a function of relative humidity.

For the purpose of this analysis, the contact configuration between the particles of a compact during stress relaxation is assumed to be equivalent to the microindentation configuration of single crystal. Therefore, the contact area derived from the microindentation tests can be used to normalize the deformation kinetic data for tablets of different relative densities as described below (Duncan-Hewitt, 1989). This assumption

has been shown to give rise to activation parameters that agree with those calculated from other approaches in the cases of sodium chloride and potassium bromide. In addition, constancy of interparticulate contact area during the stress relaxation of PMMA copolymers has been assured microscopically (Lum, S., thesis, in progress). The assumption may still be problematic in the present work, since surface plasticization due to the presence of adsorbed water may significantly alter the deformation pattern of sucrose.

The constant area assumption is used in the following way to calculate interparticulate stress. In stress relaxation, a defined initial load is applied and the force is measured continually for an extended period. It is assumed that while compaction serves to change the interparticle contact area, once the punch movement is arrested there is no further driving force for this process. Instead, a decrease in stress occurs during stress relaxation due to the interchange of elastic and plastic strain within the large zone of deformation underlying the contact zone. The contact area is assumed to remain constant as a result. To calculate the interparticulate stress, one would need to quantitate this interparticulate contact area.

In a microindentation test, a load is lowered onto the surface of a test specimen and is allowed to remain there to increase the contact area. The load and final ten-second contact area are measured and together these measurements permit the hardness to be calculated (Papadimitropoulos and Duncan-Hewitt, 1992). If we can approximate the first ten seconds of relaxation with the first 10 seconds of indentation (once the indenter load has been fully transferred to the specimen), then the contact areas in the two processes should be approximately equal at 10 seconds. Of course, the configurations are *not* the same in geometry, but the approximation has worked in several instances as discussed above.

The model predicts that if the load is varied, the true ten-second contact area should change proportionally in both microindentation and stress relaxation. If this is the case, then one should be able to cause superimposition of the stress relaxation curves for tablets at *any* relative density by normalizing them with the 10 second contact areas.

2.1.3. The Rationale of the Microindentation Technique Applied to This Model

Microindentation is employed in this study to determine the contact area. Microindentation is advantageous for the study of the plastic deformation of brittle and semi-brittle materials because it can provide information about the brittle nature of crystals using very small loads. In microindentation tests, fracture is suppressed by the relatively high compressive hydrostatic stress associated with this test configuration and the change in the absolute strain is very small. In hardness studies of semi-brittle materials, a unique advantage has been shown in investigating the effect of hardness on mechanical behavior, and the relative effects of temperature, impurities and dislocation mobility. During this process, a diamond indenter of a specific geometry is pressed, at right angles, into the surface of the material under a given load and the area of the permanent impression is determined (Westbrook and Conrad, 1973; Duncan-Hewitt, 1988).

The two indenters that are employed most frequently are the rhombic-asymmetrical Knoop and pyramidal Vickers. The contact area is very important in this techinque, as it is used to derive the hardness of single crystals and can be used to correlate tablet stress relaxation with deformation kinetic analysis. Knoop hardness is not directly comparable to Vickers hardness because the projected area, and not the contact area is used to determine the stress. Therefore, the Vickers configuration will be employed in the

present study.

The relationship between the hardness and the shear stress for sucrose is calculated on the basis of the von Mises yield criterion (Duncan-Hewitt, 1989).

$$\tau = H / 3\sqrt{3} \qquad (38)$$

Where: τ is the shear stress and H is the hardness of the material to be indented.

2.2.1. Crystal Preparation:

Small crystals of sucrose were sieved to obtain a narrow particle size (0.600-0.425 mm) fraction for compaction testing. Larger crystals of sucrose (about 1-4mm) prepared by slowly evaporating from a 75% methanol saturated solution at about 23°C for three months were selected for the hardness test. Samples of sucrose crystals were stored over Drierite (Mallinckrodt Specialty Chemicals Company USA) in a desiccator and dried in an oven at 60 °C for one week.

The initial moisture content of the sucrose was determined by USP XXII Method III(USP XXII, 1990). (In this approach, the material is dried for 16 hrs at 105 °C.

2.2.2 Water Vapour Sorption of Crystals:

Three grams of dried sucrose samples were weighed accurately and spread on a series of tared and numbered weighing dishes and then placed into labeled desiccators. Seven sealed desiccators, each of them containing samples and one type of saturated salt solution (Table 2.2.2.1), were stored at 27 °C (in an environmentally controlled room) until no change in weight was detected. The samples exposed to relative humidity less than 80% were stored for more than two weeks to allow them to equilibrate at varying levels of relative humidity (Fig. 2.2.2.1). However, crystals exposed to air near the deliquescence point of sucrose (R.H.=84%) were stored for a week (R.H.=82%).

The various relative humidities and temperatures employed are described in Table 2.2.2.1.

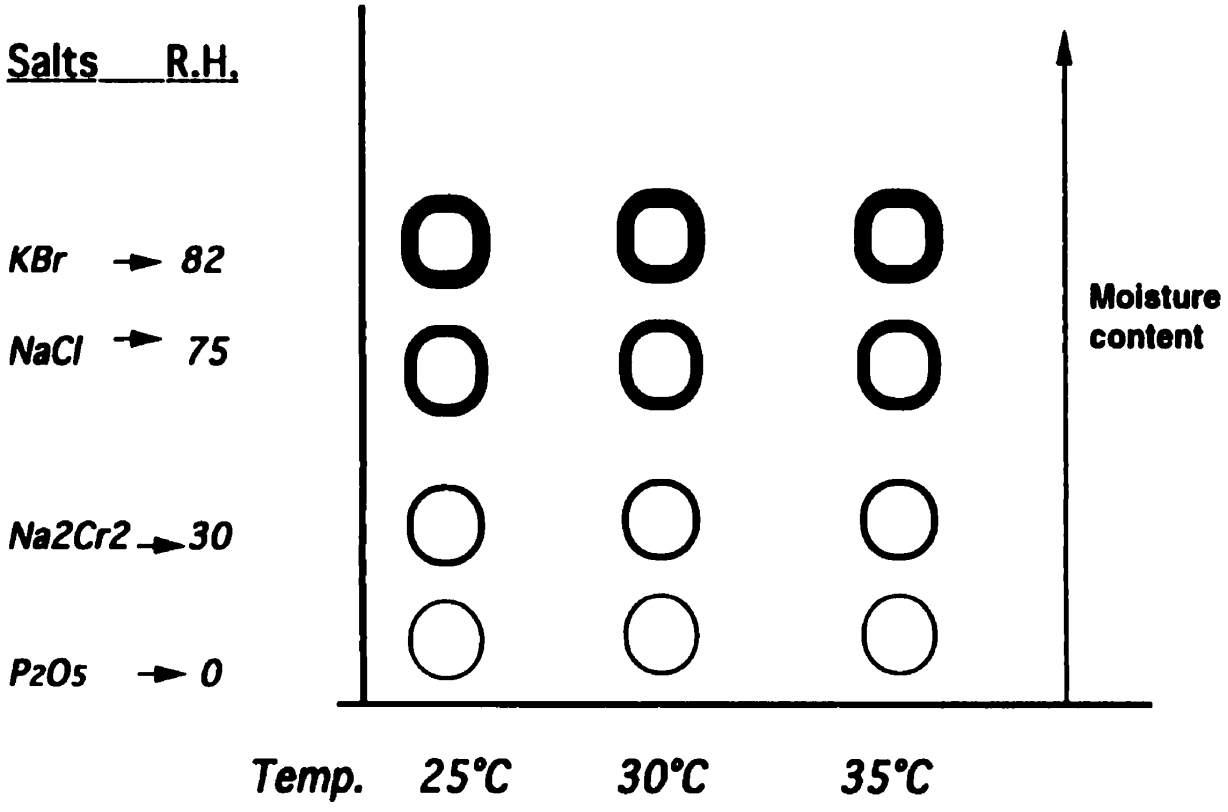

Fig. 2.2.2.1. Schematic illustrates the development of different amounts of moisture on sucrose crystal.

2.2.3. Vickers Hardness Test

Equipment: Large crystals of sucrose (1-4 mm) with known equilibrium moisture contents were prepared as described above for the microindentation test. A Tukon Miniload microindentation hardness tester (Model 300) equipped with a 136° Vickers diamond pyramid indenter and a 40 x objective for hardness testing were employed. Microindentation testing was performed under the same relative humidities and temperatures as the samples treated before. The relative humidities were controlled by AtmosBag™ containing the same saturated salt solutions. Temperature was controlled by connecting the stage to a temperature controlled bath (ULTRATEM 2000, VC thermostated circulator). The R.H. and temperature were monitored respectively by using a hygrostat and an OMEGA thermocouple.

Method: A crystal was mounted in a thermally conductive paste so that the surface (100 or 001) (Fig.2.2.3.1) to be indented was normal to the indentation direction. Normality was achieved by maximizing the intensity of the light reflected from the sucrose when the crystal was viewed under the microscope attachment and assuring the the two diagonals of the indentation were of equal length. The 40X objective was then used to select an indentation site.

2.2.4. Tablet Compaction.

Equipment: an Instron stress-strain analyzer (model 4201) equipped with series IX computer software (version 6.02C), and 12.60mm diameter stainless steel die and punches, were used for tablet compaction and the measurement of stress relaxation. The temperature and relative humidity were controlled using an environmental chamber. The

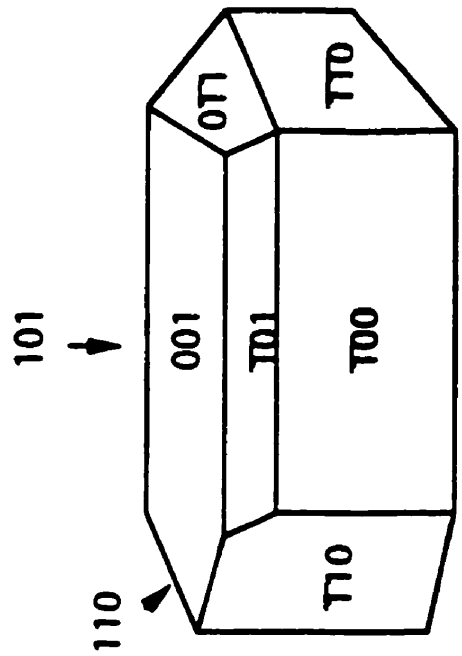

Fig.2.2.3.1 . Habit of large, prismatic crystals of sucrose

respectively. Compact thickness was measured using a digital micrometer.

Method: The die and punches were lubricated with a slurry of magnesium stearate in methanol before each compression. The die was filled with 1g* of sucrose with various levels of equilibrium moisture. The assembled die was placed on the lower platform of the Instron, and the crosshead was lowered until a compressive force of 0.01 N was measured. The crosshead was then lowered at 1mm/min until a maximum compressive force of either 4.5 or 3.0 N was attained at which point the movement of the cross-head was arrested and stress relaxation was monitored for two minutes after compaction at various designated temperatures (30° C, 35° C, 40° C, 45° C) and relative humidities (0; 55; 67; 75; 82; 88). The temperature and relative humidity were controlled using an environmental chamber (45x30x12 inch). At least three runs were performed for each set of environmental conditions.

* the filling amount was adjusted by correcting the moisture content to: 1x100/(1-∂). where: ∂ is a corresponding moisture content (%) of the sucrose.

CHAPTER THREE

RESULTS AND DISCUSSION, REMARKS AND CONCLUSIONS

3.1. RESULTS AND DISCUSSION

3.1.1. Water Sorption of Sucrose

Exposure of sucrose crystals to increasing levels of humidity at 27.5 °C (R.H. 67% at 20 °C) caused the material to take up moisture to a varying extent (Figure 3.1.1.1). In accordance with the experimental results reported by Callahan *et al.*,1982, the equilibrium moisture content of sucrose crystals remained essentially constant until a relative humidity beyond 67% then began to increase dramatically. These results also are supported by Panacoast and Junk (1980) who reported that the moisture content of sucrose increases exponentially once the relative humidity exceeds 60%.

3.1.2. Relationship Between Relative Humidity, Temperature and Sucrose Crystal Hardness

From Figure (3.1.2.1), it can be seen that increasing the relative humidity from 0% to 56% corresponds with no significant change in crystal hardness. However further increases of the relative humidity beyond this point resulted in a marked reduction in the crystal hardness. This may arise due to the water-induced disruption of the hydrogen bonds cross-linking the hydroxyl groups on the sucrose chains causing the sucrose to become "plasticized" (Pilpel and Ingham, 1988; Kristensen *et al.*, 1985; Ahlneck and Alderborn, 1989).

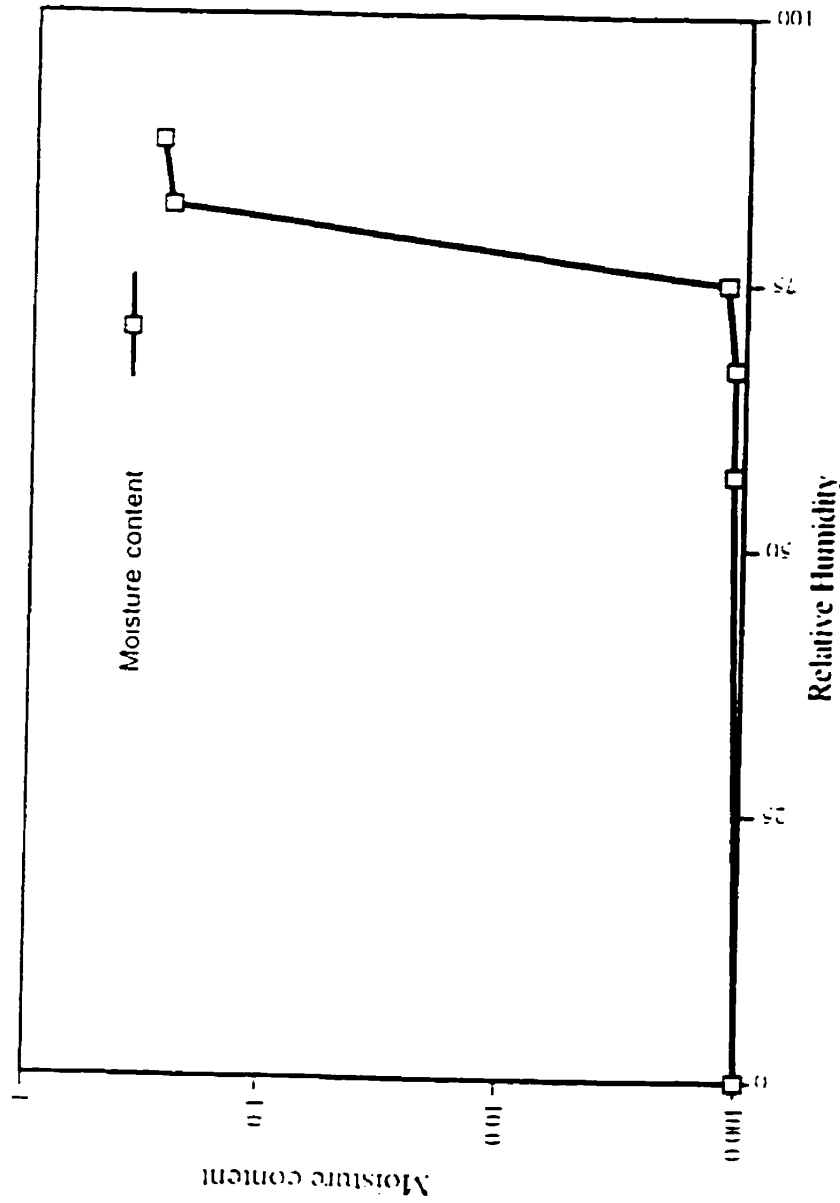

R.H.(%)	0	55	67	77	82
No.of Tested Samples	12	12	12	10	10
Moisture content (g/g DSB)	0.0014 ± 0.0001	0.0014 ± 0.0001	0.0014 ± 0.0001	0.0024 ± 0.0001	0.2564 ± 0.0002

Fig.3.1.1.1. Sucrose Water Vapor Sorption (g/g) vs relative humidity (%)

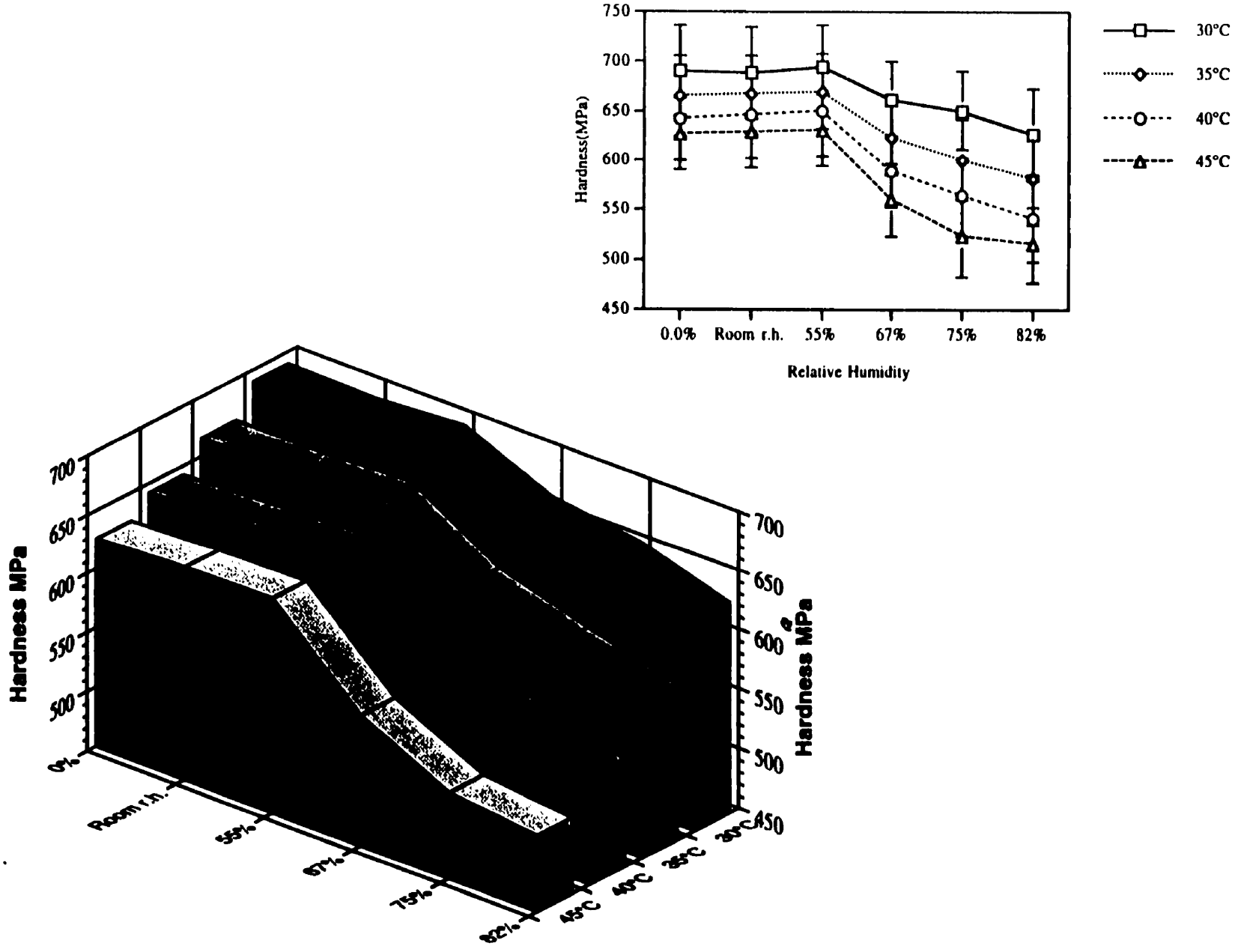

Fig. 3.1.2.1. Hardness (mean±std) of sucrose single crystals plotted as a function of relative humidity and temperature

The hardness was observed to decrease (Fig. 3.1.2.1) with increasing temperature. This observation is expected since the hardness of a material is a measurement of the constrained resistance to plastic deformation which is controlled by thermal activation. Increasing the temperature causes the average internal energy of the molecules to increase, so that more molecules achieve the activation energy which, in turn facilitates viscous flow.

3.1.3. Relationship Between Relative Humidity, Temperature, Activation Volume and Activation Energy.

Activation Volume

The plots of ln (shear stress rate) vs shear stress (Fig.3.1.3.1) for the stress relaxation of sucrose compacts compressed at lower temperatures and relative humidities exhibit a linear relationship between shear stress rate and shear stress ($r^2>0.99$ see Appendix I) suggestive of only one mechanism with a single-energy barrier that is rate controlling. The activation volumes for sucrose calculated using Eq. (29) are summarized in Table 3.1.3.2.

The results indicate that, for these linear cases, the activation volume ranged from about $3b^3$ to $6b^3$ (Table 3.1.3.2) suggesting that the rate may be controlled predominantly by a climb mechanism (Krausz and Eyring, 1975) which is a thermally activated process requiring mass transport by diffusion. While these results are of the same order as those obtained by a microindentation creep method, they are about twice the magnitude (Duncan-Hewitt, 1989). The implication is that during the relatively short time period of

stress relaxation, a larger volume of material is affected than during slow processes such as creep. This finding is not in accord with the behavior of many materials. As the strain rate decreases, the deformation tends to shift towards mechanisms with higher, not lower, activation volumes.

Some of the plots of ln (shear stress rate) vs. shear stress (For example Fig.3.1.3.1) obtained for the stress relaxation data derived for relative humidities ranging from 67% to 82% are not linear but are distinctly curved ($r^2<0.99$, see Appendix I) so a linear model is not adequate to describe the behavior of the material under these conditions. A thorough investigation of the experimental results proved that a much better fit was provided by a model with two barriers combined in series using Eq. (22) (Fig. 3.1.3.3). Neither the parallel system kinetics or a single nonsymmetrical energy barrier sufficed (evaluation based on Eq. (19) , see Fig. 3.1.3.2).

Using the two-barrier-series model, the activation volume obtained for the first barrier was 4 b^3-6 b^3 while the combination of the first and second barrier ranged from 6b^3 to 30 b^3, indicating that climb mechanisms still predominate at higher stresses, but that a Peierls-Nabarro mechanism predominates at lower stresses.

Activation Energy

The apparent activation energies at different relative humidities are calculated using Eq. (28) and summarized in: Table 3.1.3.3.

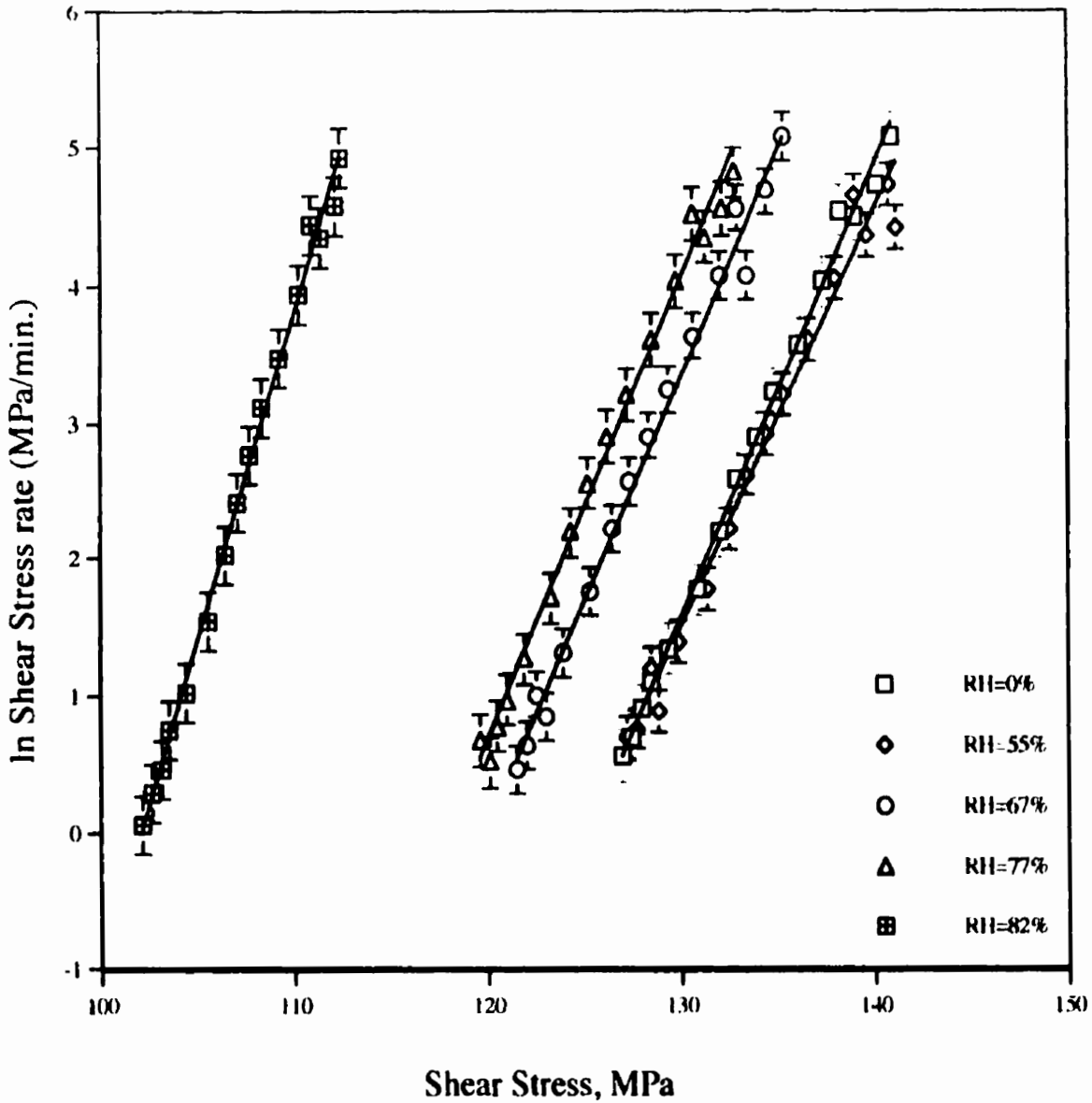

Fig.3.1.3.1 a The ln (shear stress rate) versus shear stress plots with error bars (mean±STD) for the stress relaxation for sucrose compacts compressed at 30°C and different relative humidities.

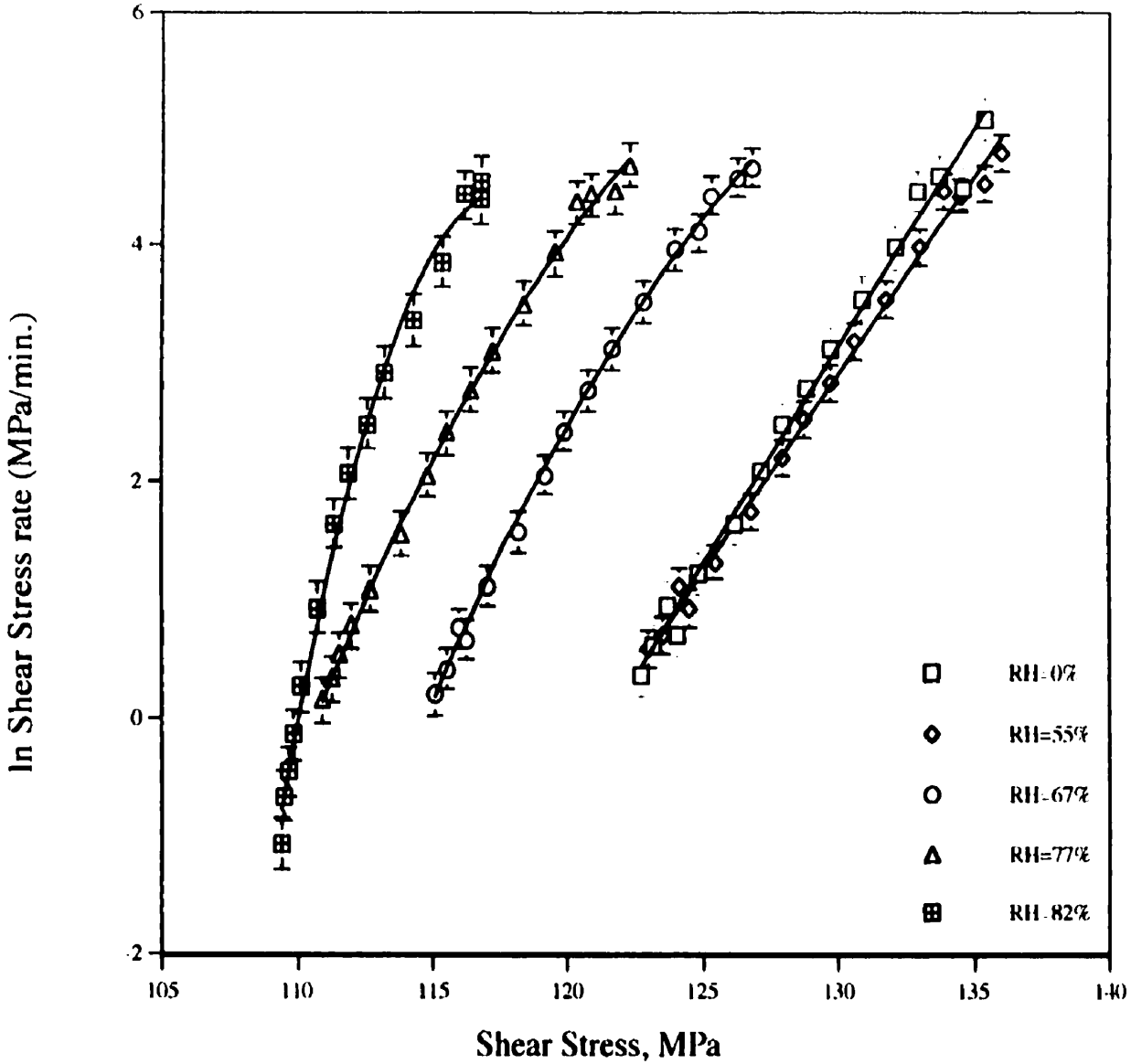

Fig.3.1.3.1b The ln (shear stress rate) versus shear stress plots error bars (mean±STD) for the stress relaxation for sucrose compacts compressed at 35°C at different relative humidities.

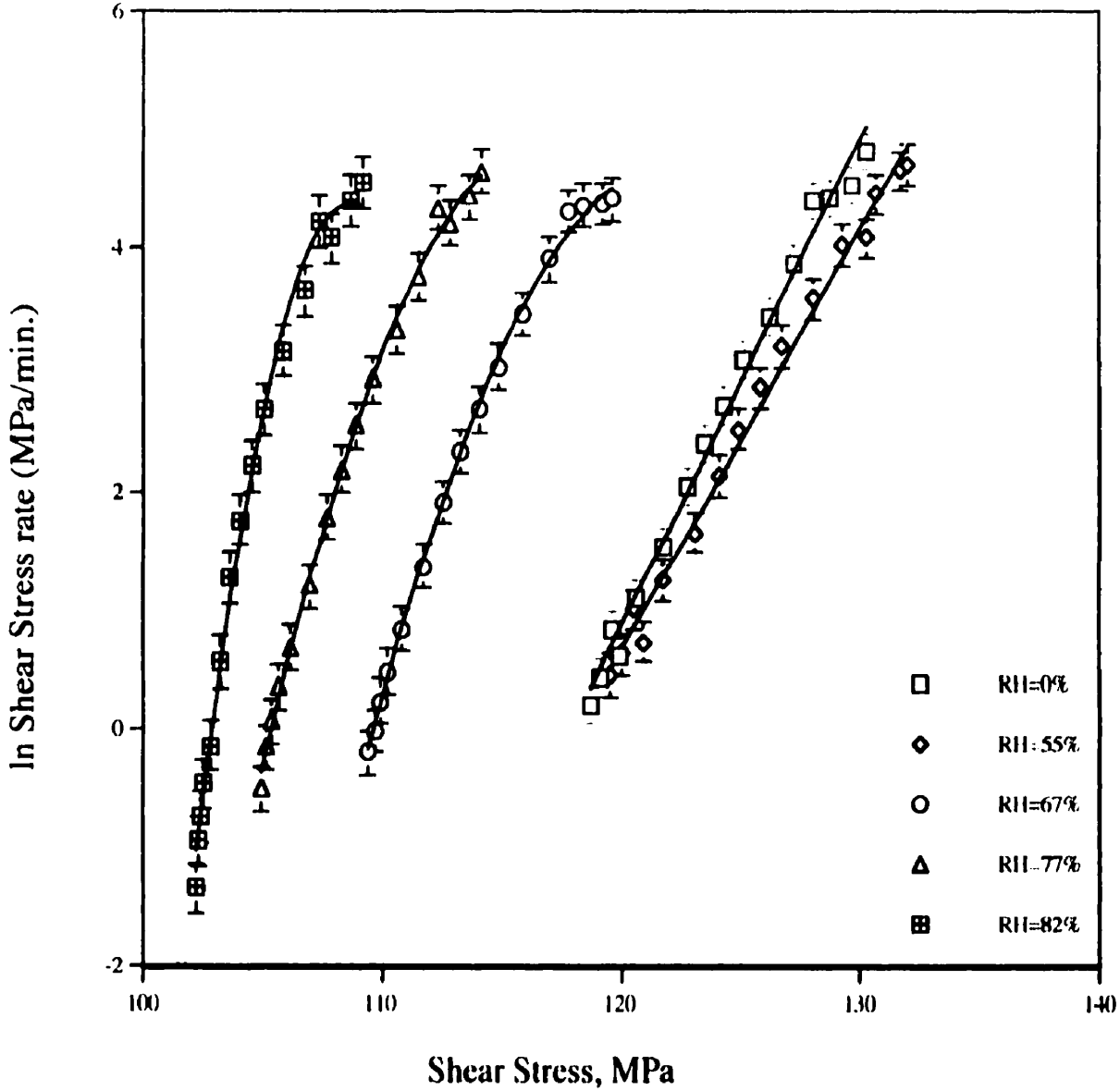

Fig.3.1.3.1 c The ln (shear stress rate) versus shear stress plots with error bars (mean±STD) for the stress relaxation for sucrose compacts compressed at 40°C and different relative humdities.

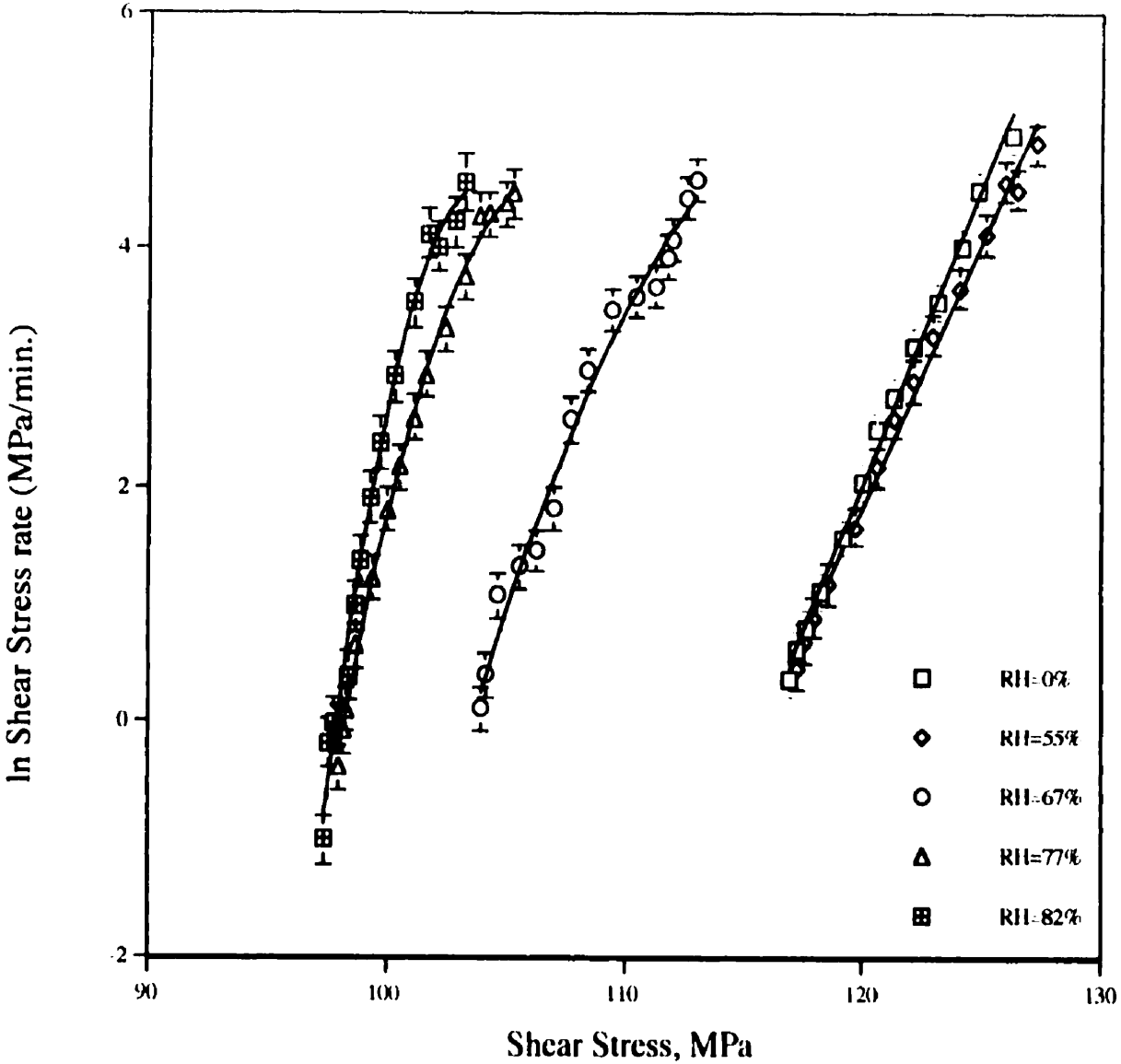

Fig.3.1.3.1 d The ln (shear stress rate) versus shear stress plots with error bars (mean±STD) for the stress relaxation for sucrose compacts compressed at 45°C and different relative humidities.

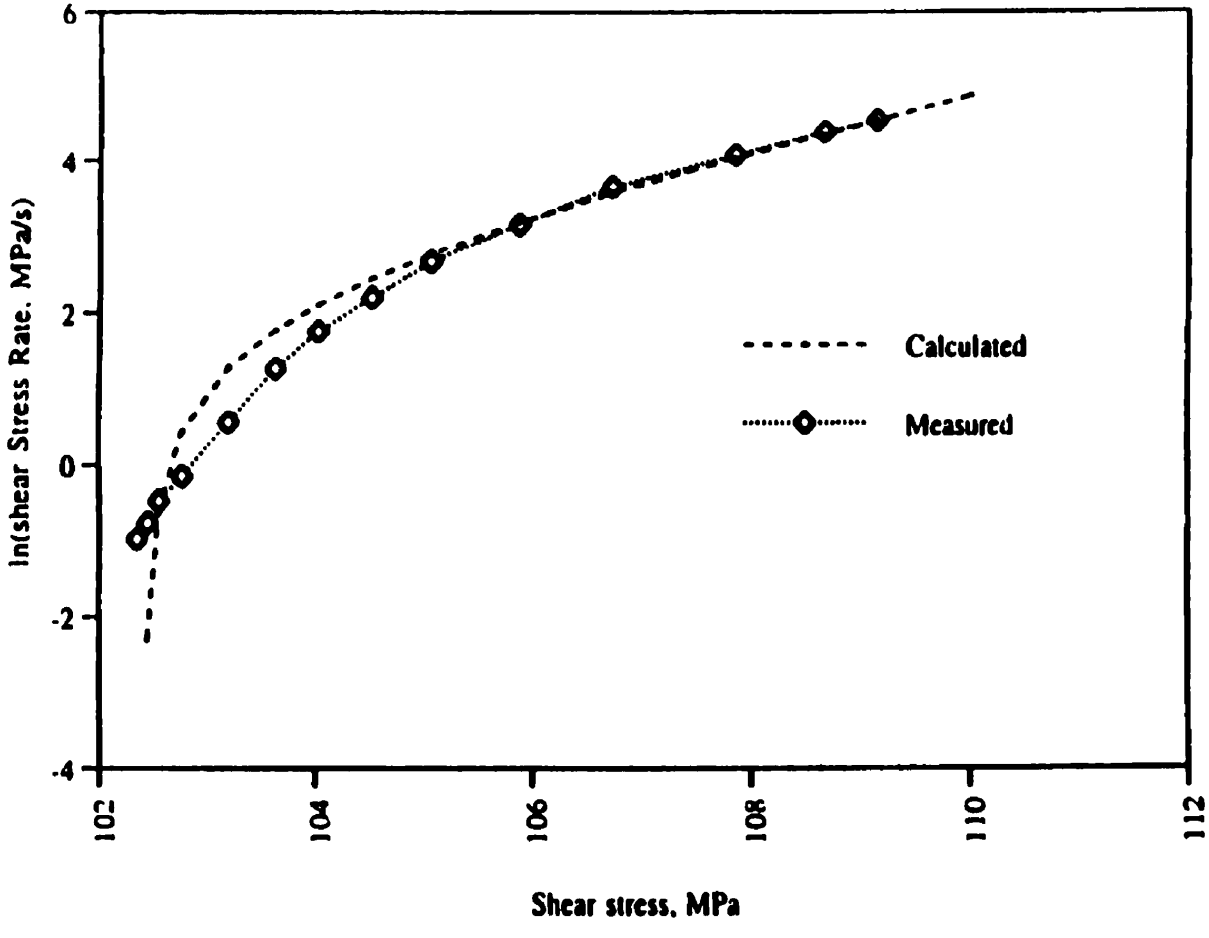

Fig.3.1.3.2. Typical plot of ln (shear stress rate, MPa/s) versus shear stress for the stress relaxation of sucrose compacts compressed with maximum loads 4.5KN at r.h. 82 and temperature 40°C. The measured data does not match the calculated data from the single nonsymmetrical energy barrier kinetic equation $\dot{\gamma}=\delta_1\rho_n A_n \exp(-V_{b1}\tau/kT_1)-\delta_1\rho_{b1}A_{b1}\exp(-V_{b1}\tau/kT)$

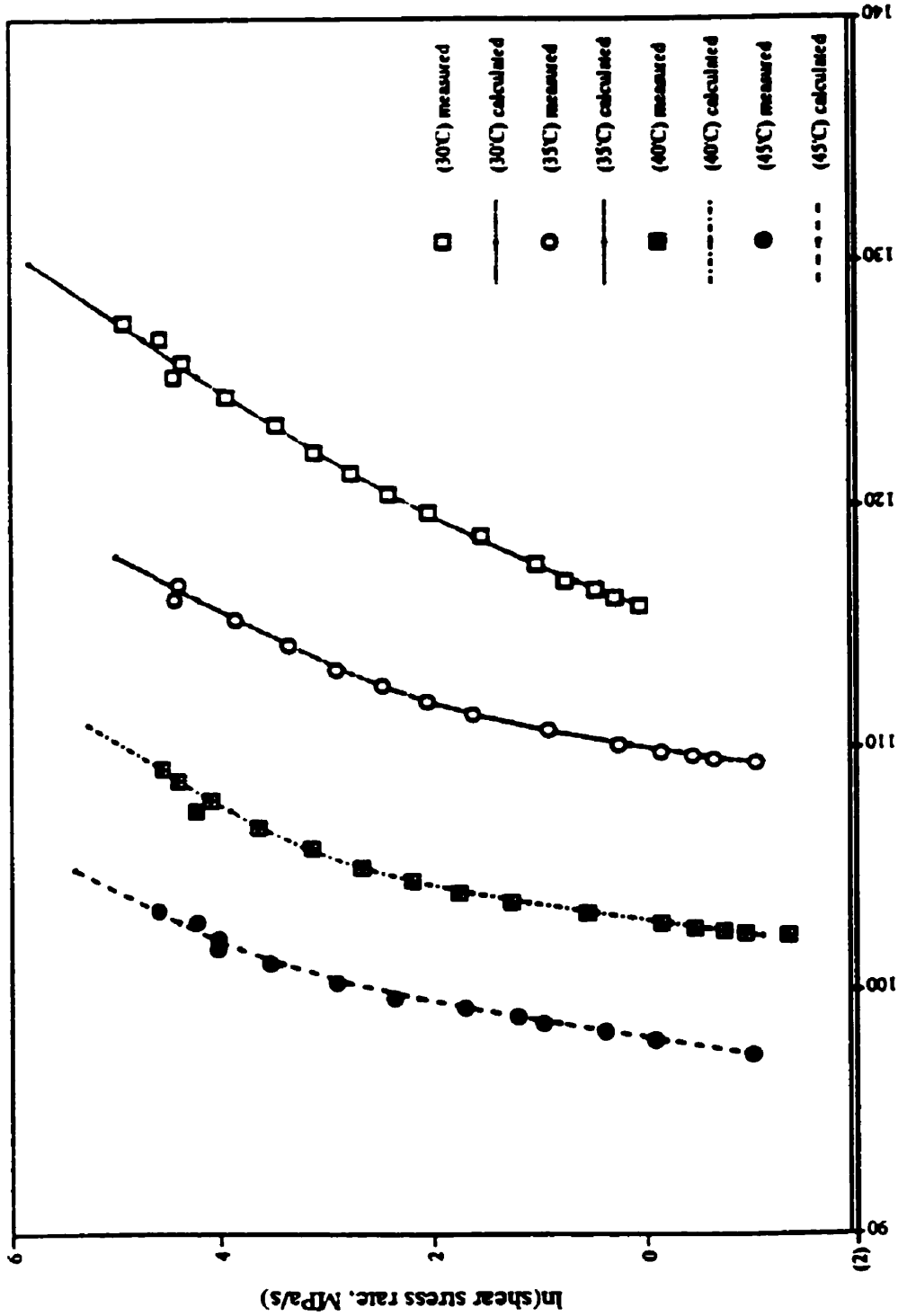

Figure 3.1.3.3. Typical plots of ln (shear stress rate, MPa/s) versus shear stress for the stress relaxation of sucrose compacts compressed with a maximum load 4.5 kN at r.h 82 at various temperature. The fit obtained using eq.22 was excellent.

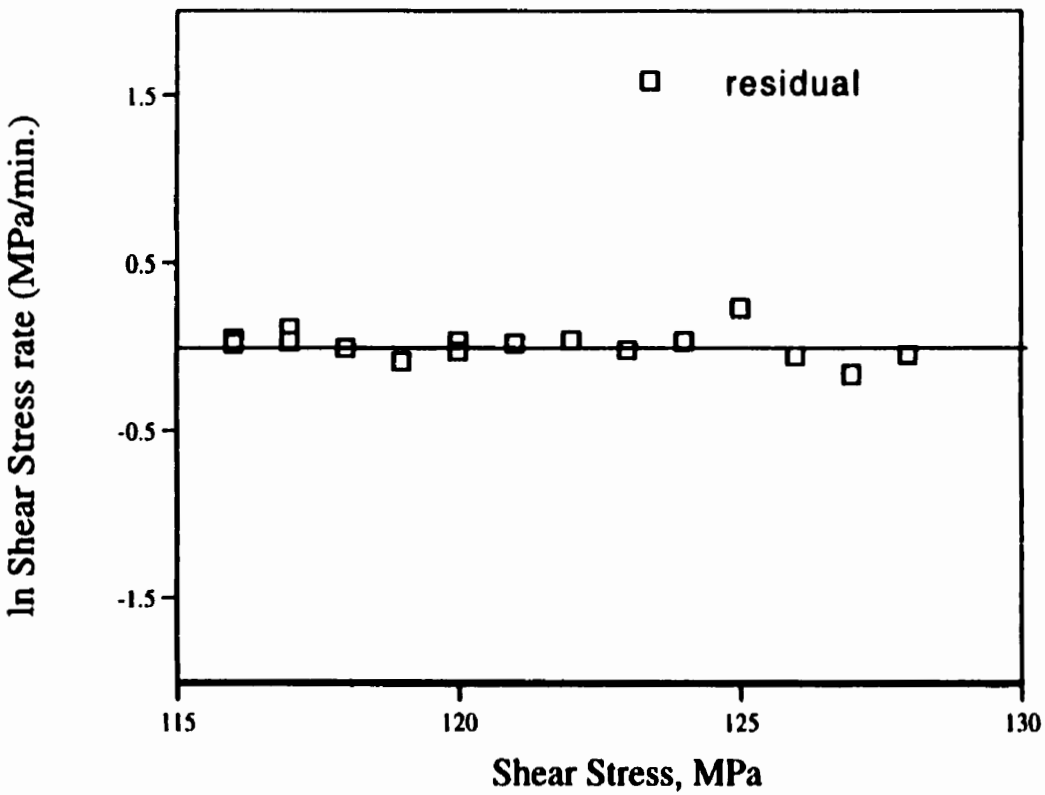

Figure 3.1.3.3a. Plot for the residual of ln (shear stress rate, MPa/s) versus shear stress and its fitted curve obtained using eq.22 at r.h 82 and 30°C. The residual values are randomly scattered around 0 indicate that the fiting is accepted

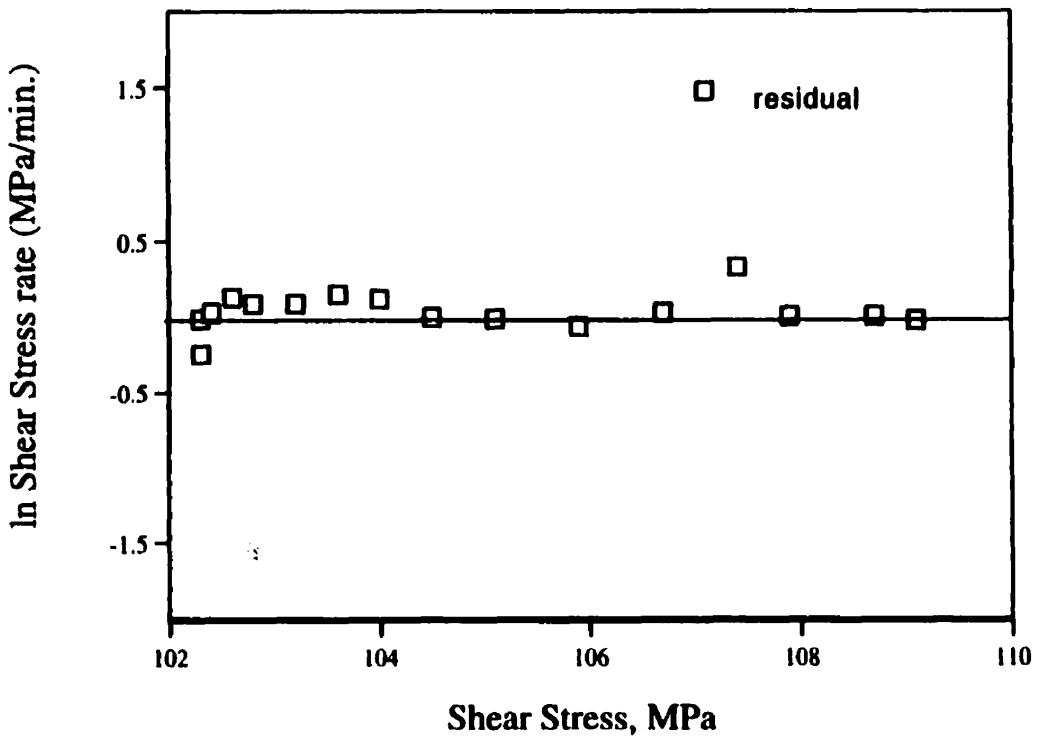

Figure 3.1.3.3c. plot for the residual of ln (shear stress rate, MPa/s) versus shear stress and its fitted curve obtained using eq.22 at r.h 82 and 40°C. The residual values are randomly scattered around 0 indicate that the fiting is accepted

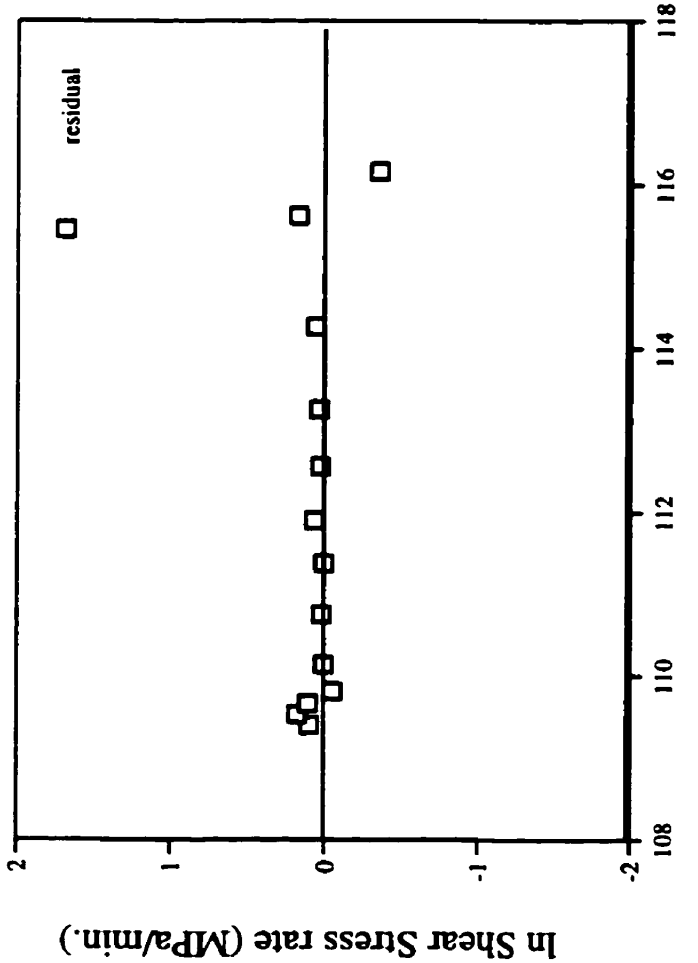

Figure 3.1.3.3b. plot for the residual of ln (shear stress rate, MPa/s) versus shear stress and its fitted curve obtained using eq.22 at r.h 82 and 35°C. The residual values are randomly scattered around 0 indicate that the fiting is accepted

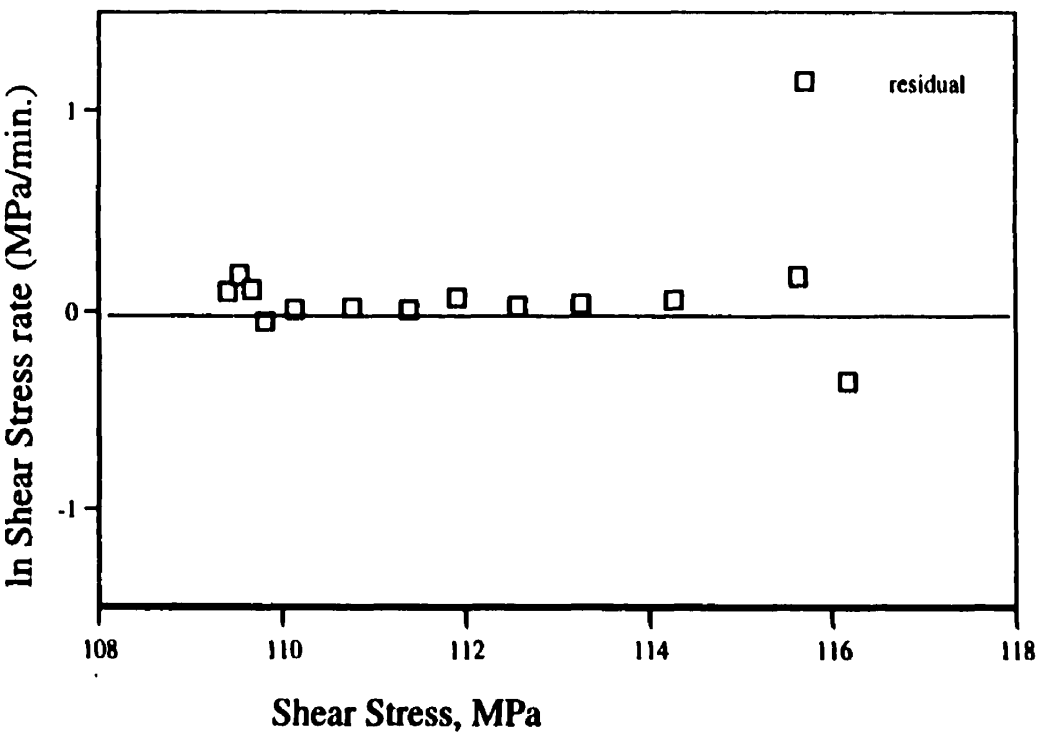

Figure 3.1.3.3d. plot for the residual of ln (shear stress rate, MPa/s) versus shear stress and its fitted curve obtained using eq.22 at r.h 82 and 45°C. The residual values are randomly scattered around 0 indicate that the fiting is accepted

	0%	55%	67%	77%	82%
Temp.30 C	3.8±0.0	3.6±0.1	3.8±0.1	3.9±0.0	3.9±0.0a 10.1±0.1b
Temp.35 C	4.5±0.1	3.9±0.1	4.21±0.2a 6.95±0.6b	3.6±0.1a 8.2±0.7b	5.2±0.1a 30.3±0.5b
Temp.40 C	4.8±0.1	4.3±0.2	4.6±0.1a 15.5±0.3b	3.9±0.2a 17.4±0.3b	4.5±0.0a 27.5±0.5b
Temp.45 C	5.7±0.1	5.4±0.2	4.7±0.3a 27.6±0.7b	6.9±0.2a 29.7±0.4b	5.4±0.1a 29.1±0.9b

a: represents the first barrier $V_{f1;}$ b: representive the combination of the first and second barrier $V_{b1}+V_{f2}$

Table 3.1.3.2. Summary of activation volume (b^3) (mean±S.E. n=3) at varying relative humidities and temperatures

Table 3.1.3.3. Activation Energies • (mean±S.E. n=3) at different relative humidities

Relative Humidity	Activation Energy For First Barrier ($kJ \cdot mol^{-1}$)
0%	228.7±7
55%	203±11
67%	375±11
77%	528±125
82%	627±61

•calculation see Appendix II.

The activation energy for a sucrose compact at lower relative humidity was about twice that determined by the indentation creep method used for a single crystal by Duncan-Hewitt (1989) which itself was somewhat high, although within the range of those of similar materials when normalized by the melting temperature.

At ambient conditions, the sucrose compacts deformation process is controlled by two consecutive energy barriers as discussed before. The first energy barrier predominated at a higher stress range. The activation energies were calculated by using Eq. 28 and are summarized in Table 3.1.3.3. As the stress decreased during relaxation, the effects of a second barrier became apparent which were estimated to be 20% greater than the first barrier. The energy profiles of the present analysis are in agreement with the report of Hanley *et al.* 1973. Given the *softness* of the material (similar to iron), an activation energy as high as the one determined in this study gives rise to doubts about its accuracy.

3.2. REMARKS ON THE MODEL SYSTEM FOR BRITTLE MATERIAL UNDER AMBIENT CONDITIONS

Before closing this chapter, the model systems will be further explored. Since there is a lack of confidence in the activation energy determinations, it makes sense first to explore the potential reasons for a discrepancy between the expected and measured activation parameters, assuming that all measurements were made correctly.

(1) Faster mechanisms, responsible for most of the deformation, may not be operating when the measurements begin (at least 1 s after the punch movement is arrested);

(2) The model that links indentation and stress relaxation may not be correct for brittle material under ambient conditions.

That either of these problems might be the source of the unexpected results seemed improbable when this study was designed because the approach yielded activation parameters for sodium chloride and potassium bromide that were statistically indistinguishable from parameters determined by other methods -- including microindentation (Papadimitropoulos and Duncan-Hewitt, 1992; Frost and Ashby 1982). However, it may be that the study was complicated by the fact that it has been shown that sucrose densifies by a different mechanism than the materials studied previously.

3.2.1. Brittle and Ductile Model Materials

In attempts to model the compaction of sucrose and sodium chloride, Duncan-Hewitt (1988) found that two distinct compaction models were required to explain the differences in their behaviors. Sucrose, as a brittle material, undergoes extensive fracture

It was found that shear stresses played a role in the densification of both materials, but in different ways.

The more ductile particles have been shown to become blunted and rounded during compaction. Shear stresses caused by the imbalance of the punch and diewall stresses cause expansion of the interparticulate contact regions so that the net interparticulate contact stress is lower than the hardness. On the other hand, the more brittle particles remain angular and tend to crush at their contacts. Densification occurs as a result of a combination of this crushing and particle rotation.

The assumption was made that once the punch movement ceases that both ductile and brittle compacts behave in the same way. That is, the punch and die-wall stresses equalize very rapidly by a combination of relaxation in the direction normal to the punches and a *continued increase in stress in the direction normal to the diewall.* Once a hydrostatic state is reached, then the interparticulate stress would be best approximated by the particle hardness during the rest of the relaxation period. That the activation parameters for sodium chloride and potassium bromide were well-estimated by the calculations was based on the foregoing assumptions.

On the other hand, the stress in the sucrose compact relaxed much more quickly than expected. *This might happen if the particles continued to rotate during the relaxation period.* If rotation occurred, then the interparticulate contact area would continue to enlarge and the model would be invalidated. This hypothesis could be tested by examining the relative increase in strength and relative density of sucrose and sodium chloride tablets as a function of relaxation time.

3.2.2. Validation of this Model Under Ambient Conditions

The model of tablet stress relaxation (Papadimitropoulos and Duncan-Hewitt, 1992) was developed in order to normalize the tablet stress relaxation curves so that their kinetic analysis would be independent of porosity. It was hypothesized that if the model used for the normalization was correct, the relaxation curves would be superimposable regardless of the initial compaction stress.

In the present study, the stress relaxation curve for sucrose compacts under ambient conditions are complex (Fig.3.2.2.1). At higher stress and drier environment, the relaxation curve for compacts of different relative densities still superimposed and fit the model well. However, at lower stresses and higher relative humidity the relaxation curve for compacts of different relative densities gave poor overlap, probably due to dislocation tangles or interaction causing strain hardening. Similar observations were found when KBr was employed as model material (Papadimitropoulos, 1990).

One would have expected to observe a much lower activation energy at higher relative humidities than were actually observed. It may be that the relaxation of hydrated sucrose was so fast that its effect was buried in the very first few points of the relaxation curves.

3.3. CONCLUSIONS BASED ON THE MODEL SYSTEMS USED IN THIS STUDY.

The effect of moisture on the consolidation and compaction properties of sucrose has been investigated by applying the model established in this project. The model has

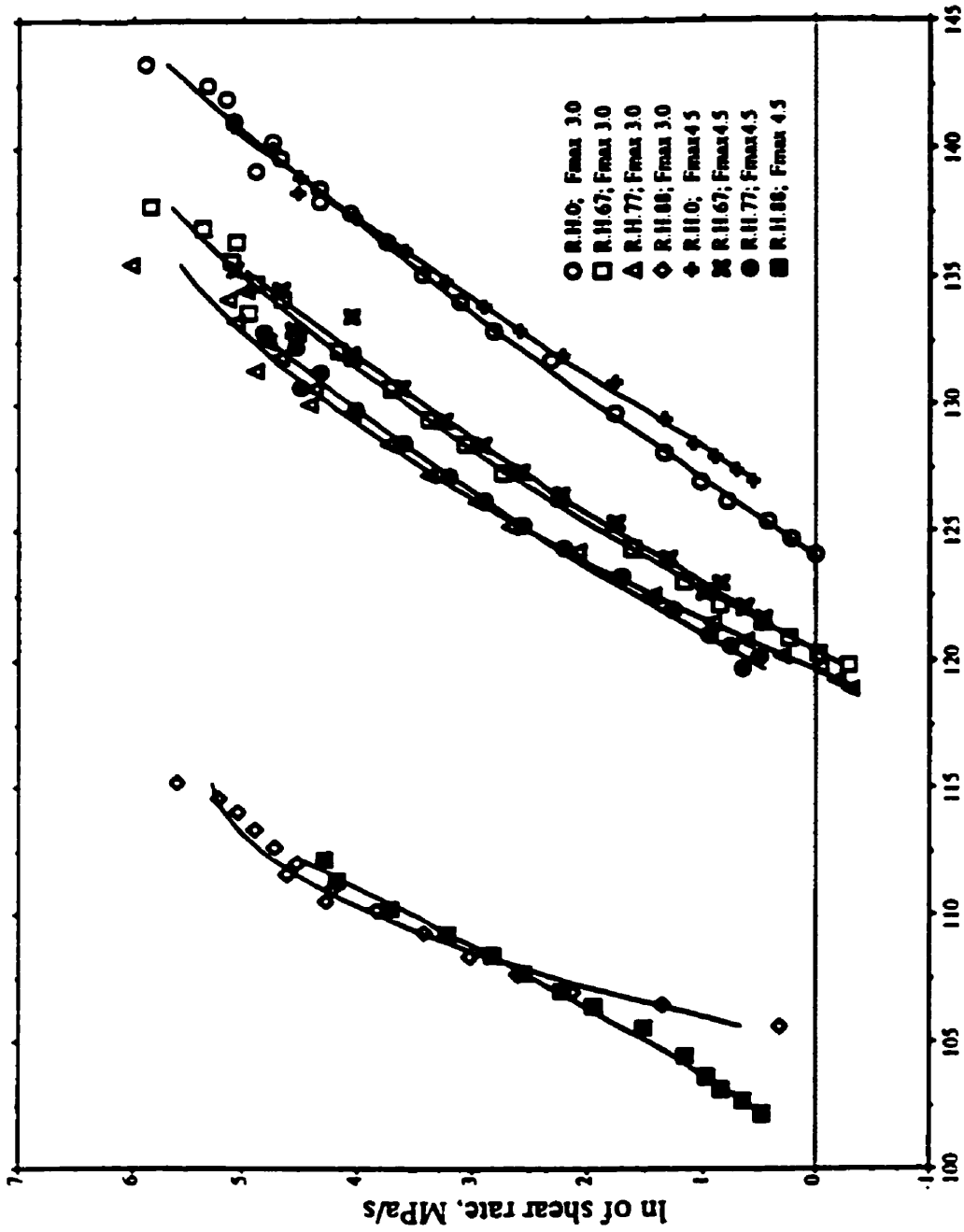

Figure.3.2.2.1. Plots of ln (shear stress rate) versus shear stress for the stress relaxation of sucrose compacts compressed with maximum load of 3.0kN and 4.5kN. at four different relative humidities

proved to be a valuable tool in assessing the visco-elastic characteristics of pharmaceutical compacts. The aspects of success or lack of success with this model have also been discussed.

This study has shown that the hardness of a sucrose particle markedly decreased when relative humidity increased beyond 67%. The study also indicated that when the sucrose crystals were equilibrated in a drier environment (relative humidity below 55%), the deformation barriers of sucrose compacts were symmetrical at equilibrium with a single energy barrier and controlled by the climb mechanism. Moreover, a thorough investigation of the experimental results showed that the stress relaxation process of sucrose compacts was controlled by two consecutive barriers at ambient conditions (relative humidity between 67% to 82%). The climb and Peierls-Nabarro mechanisms were found to be associated with these barriers.

Both success and failure of this model provide impetus for attempting to predict more complex situations. The present study is only one part of a systematic approach to the goal that most formulation problems may be predicted and overcome based on the measurement of a few mechanical properties of single crystals.

REFERENCES:

Ahlneck, C. and Alderborn, G., *Moisture adsorption and tableting. I. Effect on volume reduction properties and tablet strength for some crystalline materials,* Int. J. Pharm., **54**:131-141 (1989).

Alderborn, G. and Ahlneck, C., *Moisture adsorption and tableting, III. Effect on tablet strength-post compaction storage time profiles,* Int. J. Pharm., **73**:249-258 (1991).

Armstrong, N.A., *Time-dependent factors involved in powder compression and tablet manufacture,* Int. J. Pharm., **49**:1 (1989).

Armstrong, N.A. and Griffiths, R.V., *Surface area measurements in compressed powder systems,* Pharm. Acta. Helv., **45**:583-591 (1970).

Armstrong, N.A., and Patel, A., *The compressional properties of dextrose monohydrate and anhydrous dextrose of varying water contents*, Drug Dev. In. Pharm., **12**:1885-1901 (1986).

Aulton, M.E., *Indentation hardness profiles across the faces of some compressed tablets*, Pharm. Acta Helv., **56**:133-136 (1981).

Aulton, M.E., *Micor-indentation tests for pharmaceuticals,* Manuf. Chem. Aerosol News, **48**:28-31 (1977).

Banqudu, A.B. and Pilpel, N., *Effect of composition, moisture and stearic acid on the plastic-elasticity and tableting of paracetamol-microcrystalline cellulose mixtures.* J. Pharm. Pharmacol., **37**:289-293 (1985).

Banker, G.S. and Rhodes C.T., *Modern Pharmaceutics*, second edition (1990).

Barraclough, P.B. and Hall, P.G., *Adsorption of water vapor by lithium fluoride, sodium fluoride and sodium chloride.* Surf. Sci., **46**:393-417 (1974).

Beevers, C.A., McDonald, T.R.R., Robertson, J.H., and Stern,F., *Crystal structure of sucrose*. Acta Cryst., **5**:691 (1952).

Brown, G.M. and Levy, H.A., *Sucrose-precise determination of crystal and molecular scructure by neutron diffraction.* Science **141**:921-924 (1963).

Caddell, R.M., *Deformation and fracture of solids.* Englewood Cliffs, N.J.: prentice-Hall, (1980)

Casahoursat, L., Lemagnen, G. and Larrouture, D., *The use of stress relaxation trials to characterize tablet capping.* Drug Development and Industrial Pharmacy **14**:2179-2199 (1988).

Carstensen, J.T., *Pharmaceutics of Solid Dosage Forms*, John Wiley and Sons, New York, (1980).

Cartensen, J.T. and Li, Wan Po A., *The state of water in drug decomposition in the moist solid state: Description and modeling* Int. J. of Pharm., **83**:87-94 (1992).

Chikazawa, M. and Kanazawa, T., *Hygroscopic phenomena of water soluble salts.* Funtai Kogaku kenkyu kaishi, **15**:164-171 (1978).

Chowhan, Z.T., and Pakagyi, L., *Hardness increase induced by partial moisture loss in compressed tablets and its effect on in vitro dissolution,* J. Pharm. Sci., **67**:1385-1389 (1978).

Chowhan, Z.T., *Role of binders in moisture-induced hardness increase in compressed tablets and its effect on in vitro distegration and dissolution,* J. Pharm. Sci., **69**: 69(1): 1-4 (1980).

Danielson, D.W., Morehead, W.T. and Rippie E.G.J., *Unloading and postcompression viscolelastic stress versus strain behavior of pharmaceutical solids,* Pharm. Sci., **72**:343 (1983).

David, S.T. and Augsburger, L.L., *Plastic flow during compression of directly compressible fillers and its effect on tablet strength,* J. Pharm. Sci., **66**:155-159 (1977).

Davidge, R.W., *Mechanical Behaviour of ceramics*, Cambridge University Press,

Cambridge, U.K., 1979.

Duncan-Hewitt, W.C., *The use of microindentention techniques test the ability of pharmaceutical crystals to form strong compacts*, Ph.D. Thesis; University of Toronto, 1988.

Duncan-Hewitt, W.C. and Grant, D.J.W., *The impact fracture wear test: a novel method of tablet evaluation*, Powder Technology, **52**:17-28 (1987).

Duncan-Hewitt, W.C. Mount, D. and Yu, A. *Hardness Anisotropy of Acetaminophen Crystals*, Pharmaceutical Research, **11**: 616-623 (1994).

Duncan-Hewitt, W.C. and Weatherly, G.C. *Evaluating the deformation Kinetics of sucrose crystals using Microindentation techniques*, Pharm. Res. **6**:1060-1066 (1989).

Eaves, T. and Jones, T.M., *Effect of moisture on tensile strength of bulk solids. I. Sodium chloride and effect of particle size*, J. Pharm. Sci., **61**:256-261 (1972).

Edgar, G. and Swan, W.O., *The factors determining hygroscopic properties of soluble substances. I. The vapor pressure of saturated solutions*, J. Am. Chem. Soc., **44**:570 (1922).

Ejiofor, O., Esezobo, S. and Pillpel N., *The plasto-elasticity and compressiblity of coated powders and the tensile strengths of their tablets*, J. Pharm. Pharmacol., **38**:1-7 (1986).

Fell, J.T., and Newton, J.M., *The tesnsile strength of lactose tablets*. J. Pharm. Pharmacol., **20** (8):657-9 (1968).

Frost, H.J. and Ashby, M.F., *Deformation-Mechanism Maps*, Pergammon Press, New York, 1982.

Garr, J.S.M. and Rubinstein, M.H., *An investigation into the capping of paracetamol at increasing speeds of compression*, Int. J. of Pharm. **79**:117-122 (1991).

Garr, J.S.M. and Rubinstein, M.H., *The influence of moisture content on the consolidation and compaction properties of paracetamol*, Int. J. of Pharm. **81**:187-192 (1992).

Gebler, J. and Bauer, J., *Hardness of sucrose crystals.* Listy Cukrov., **100**:197-203 (1984).

Goodman, D. J. Frost H. J. and Ashby M. F. Phil. *The plasticity of polycrystalline ice* Philos. Mag., **43**:655-695 (1981).

Grayson, M. (Ed) *Kirk-Othmer, Silver and Siver Alloys to Sulfalones and Sulfones,* John Wiey and Sons Encycl.of Chem.Tech., 3rd Edn., Vol, 21, N.Y., 865 (1983).

Griffith, A.A., *The phenomena of rupture and flow in solids,* phil. Trans. Roy. Soc.(London), **A221**:163 (1920).

Hall, P.G. and Rose, M.A., *Adsorption of water vapour on ammonium iodide and ammonium chloride*, J. Phys. Chem., **82**:1521-1525 (1978).

Halsey, G., White, H. J. and Eyring, H., *The mechanical properties of textiles. II. A feneral theory of elasticity with application to partially rubberlike substances*, Tex. Res. J., **14**:9 (1945).

Hanley T. O'D. and Krausz A.S. *Thermally activated deformation. I; II. Method of analysis,* J. Appl. Phys., Vol. 45, No. May (1974).

Hiestand, E.N. *Tablet bond. I. A theoretical model,* Int. J. Pharm., **67**:217 (1991a).

Hiestand, E.N. *Tablet bond. II. A theoretical model,* Int. J. Pharm., **67**:231 (1991b).

Hiestand E.N., and Smith D.P., *Three indexes for characterizing of tableting peformancing of materials.* Powder Tech., **38**:145 (1984).

Hiestand, E.N., Wells, J.E., Peot,C.B., and Ochs, J.F., *Physical processes of tabletting,* J, Pharm. Sci., **66**:510-519 (1977).

Hirth, J, P., and Lothe, J., *Theory of dislocations.* McGraw-Hill, New York, (1968).

Holman L.E. and Leuenberger H., *The relationship between solid fraction and mechanical*

properties of compacts - the percolation theory model approach, Int. J. Pharm., **46**:35 (1988).

Hüttenrauch, R. and Jacob, J., *Effects of lubricants on the compression force distribution in compressed tablets.* J. Die Pharmazie, **32**:240-241 (1977).

Jetzer, W. E., *Measurement of hardness and strength of tablets and their relation to compaction performance of powders,* J. Pharm. Pharmacol., **38**:254-258 (1986).

Kaiho, M., Chikazawa, M. and Kanazawa, T., *Adsorption characteristics of water vapor on sodium chloride.* Nippon kagaku kaishi, 1386-1390 (1972).

Khan, K.A. and Pilpel, N., *An investigation of moisture sorption in isotherms and dielectric response.* Powder Technol., **50**:237-241 (1987).

Khan, K.A., Musikabhumma, P. and Warr, J.P., *The effect of moisture content of microcrystalline cellulose on the compressional properties of some formulations,* Drug Dev. Ind. Pharm. 7:525-538 (1981).

Kontny, M.J., Grandolfi G.P., and Zografi, G., *Water vapor sorption of water-soluble substances: studies of crystalline solids below their critical relative humidities.* Pharm. Res., **4**:104 (1987).

Krausz, A.S. and Eyring, H., *Deformation Kinetics*; Wiley: New York, (1975).

Krausz, A.S. and Krausz, K., International Journal of Structural Mechanics and Materials Science, **23**:99-112 (1988).

Krausz, A. S. and Krausz, K. *Deformation kinetics of plastic deformation: Physically based constitutive laws. Plastic Flow and Creep American Society of Mechanical Engineers. Applied Mechanics Division,* AMD v 135. Publ by ASME, New York, NY, USA. p79-92 (1992).

Kristensen, H.G., Holm, P. and Schaefer, T., *Mechanical properties of most agglomerates in relation to granulation mechanisms. Part I. Deformability of moist densified agglomerates,* Powder Technol., **44**:227-237 (1985).

Lawn, B.R. Wilshaw, T.R., Barry T.I. and Morrell, R. *Hertzian fracture of glass ceramics,* J. Mater. Sci., **10**:179 (1975).

Li, L.C. and Peck, G.E., *The effect of moisture content on the compression properties of maltodextrins.* J. Pharm. Pharmacol., **42**:272-275 (1990).

Lieberman, H. A., Lachman L. and Schwartz J. B. *Pharmaceutical Dosage Forms Tablets,* Vol.(I) (II) (III) New York Dekker. (1989)

Lin, M.C., *Post-consolidation behaviour of acetaminophen crystals,* M.Sc Thesis; University of Toronto, (1991)

Markowitz, M.M. and Boryta, D.A., *A thermodynamic approach to the measurement of hygroscopicity. Aqueous vapor pressure of univariant binary systems, and hygroscopicity potentia,* J. Chem. Eng. Data, **6**:16-18 (1961).

Malamataris, S., Goidas, P. and Dimitrious, A. *Moisture sorption and tensile strength of some tableted direct compression excipients* Int. J. Pharm., **68**:51-60 (1991).

Monedero Perales, M.C., *Analysis compararive of methods to evaluate consolidation mechanisms in plastic and viscoelastic materials used as direct compression excipients,* Drug Dev. & Ind. Pharm., **20**: 327-342 (1994).

Morehead T. W., *Viscoelastic behavior of pharmaceutical materials during compaction,* D. Devel. and Ind. Pharm. **18**: 659-675 (1992).

Morehead, T.W. and Rippie, E.G., *Timining relationships among maxima of punch and die-wall stress and punch displacement during compaction of viscoelastic solids,* J. Pharm. Sci., **79**: 1020 (1990).

Nabarro, F.R.N., *Theory of crystal dislocations,* Clarendo Press, Oxford, (1967)

Nyqvist, H., *Saturated salt solutions for maintaining specified relative humidities,* Int. J. Pharm. Tech. & Prod. Mfr., **4**: 47-48 (1983).

Nyström, C., Malmqvist K., Mazur, W Alex and Hölzer, A.W., *Measurement of axial and radial tensile strength of tablet and their relation to capping,* Acta Pharm. Sci., **15** (1978).

Panacoast, H.M. and Junk, W.R., *Handbook of sugars,* 2nd edn., AVI publishing Co., Westport, Conn., (1980).

Papadimitropoulos, E.A., *Post consolidation behaviour of two crystalline materials, sodium chloride and potassium bromide,* M.Sc Thesis; University of Toronto, (1990).

Papadimitropoulos, E.A. and Duncan-Hewitt, W. C., *Predicting the postconsolidation Relaxation Behavior of Sodium Chloride Tablets;* J. Pharm. Sci., **81**:701 (1992).

Peleg, M. and Moreyra, R., *Effect of moisture on the stress relaxation pattern of compacted powders,* Powder Technol., **23**: 277-279 (1979).

Pilpel, N. and Ingham, S., *The effect of moisture on the density, compaction and tensile strength of microcrystalline cellulose.* Powder Technol., **54**:161-164 (1988).

Power, B. and Dye, W.B., Agr. Food Chem. **4**:47-77 (1966).

Rees J.E. and Rue P.J., *Time-dependent deformation of some direct compression excipients,* J. Pharm. Pharmacol., **30**:601 (1978).

Ridgway, K., Shotton, E. and Glasby, J., *The hardness and elastic modululs of some crystalline pharmaceutical materials,* J. Pharm. Pharmacol., **22**:95S (1970).

Ridgway, K., Aulton, M.E., and Rosser, P.H., *The surface hardness of tablets*, J. Pharm. Pharmacol., **22**:70S (1970).

Rippie, E.G. and Danielson, D. W., *Viscoelastic stress/strain behavior of pharmaceutical tablets: analysis during unloading and postcompression periods,* J. of Pharm. Sci.; **70**:476-481 (1981).

Shangraw, R. F. Wallace, J.W. and Bowers F. M. *Morphology and functionality in tablet excipients for direct compression.* J. Pharm. Pharmacol., **30**:601 (1981).

Shangraw, R. F. Wallace, J.W. and Bowers F. M. *Morphology and functionality in tablet excipients for direct compression.* J. Pharm. Pharmacol., **30**:601 (1981).

Sheth, P., and Munzel, K., Pharm. Ind., **21**: 9 (1959).

Shukla A.J. and Price J.C. *Effect of moisture content on compression porperties of two dextrose-based directly compressible diluents,* Pharmaceutical Research, **8**: 336-40 (1991).

Thomass, J.M. and Williams, J.O., *Lattic imperfection in organic solids II. Sucrose,* Trans. Farad. Soc., **63**: 23 (1967).

Train, D. and Lewis, C.J., *Agglomeration of solids by compaction,* Trans. Inst. Chem. Eng., **40**:235 (1962).

USP XXII NF XVII. *The United states pharmacopeia The national formulary* by authority of the united states pharmacopeial convention, prepared by the committee of revision and published by the board of trustees. 1990

Van Campen, L. Zografi, G and Carstense, *An approach to the evaluation of hygroscopicity for pharmaceutical solids,* J. T. Int. J. Pharm., **5**:1(1980).

Van Campen, L. Amidon, G.L. and Zografi, G. *Moisture sorption kinetics for water-soluble substances,* J. Pharm. Sci., **72**:1381(1983) (a)

Van Campen, L., Amidon,G.L. and Zografi, G., *Moisture sorption kinetics for water-soluble substances,* J. Pharm. Sci., **72**:1388 (1983) (b)

Walter, H.U., *Adsorption von Wasser an Pulvern von Alkali halogenid kristallen vom NaCl-Typ. Z.,* Physic. Chem. N.F., **75**:287-298 (1971).

Washburn, E.W.(ed.), *International Critical Tables of Numerical Data,* Physics, Chemistry, and Technology, Volume 5, McGraw-Hill, New-York, N.Y., 216 (1926).

Westbrook, H. and Conard H.(eds.) *The Science of Handness Testing and Its Research Applications,* American Society for Metals, Metals Park, OH, (1973).

Williams, T. Morehead *Viscoelastic behaviour of pharmaceutical materials during compaction,* D. Devel. and Ind. Pharm. **18** (6&7), 659-675 (1992)

Windholz, M. Budavari S, Blumetti R.F., Otterbein The Merck index, 10th endn. Merck, Rathway, New Jersey ES (1983).

Wong, M.W.Y. and Mitchell, A. *Physicochemical characterization of a phase change produced during the wet granulation of chlorpromazine hydrochloride and its effects on tableting,* Int. Pharm. **88**:261-273 (1992).

Wray, P.E. *The physics of tablet compaction,* revised, Drug Development and Industral pharmac, **18**: 627-658 (1992).

York, P., *Solid-state properties of powders in the formulation and processing of solid dosage forms,* J. Pharm. Pharmacol., **14**:1-28 (1983).

York, P., *Analysis of moisture sorption hysteresis in hard gelatin capsules, maize starch and maize starch:drug powder mixtures,* J. Pharm. Pharmacol., **33**:267-273 (1981).

Young, F.E. and Jones, F.T., *Sucrose hydrates-sucrose-water phase diagram,* J. Phys. Coll. Chem., **53**:1334 (1948).

Zografi, G., Program and Symposia Abstracts 2nd National Meeting, American Association of Pharmaceutical Scientists, Boston (1987).

Zografi, G. and Kontny, M.J., *The interaction of water with cellulose-starch-derived pharmaceutical excipients.* Pharm. Res., **3**:187 (1986).

Appendix I

Analysis of Variance Table For for the shear stress rate-shear stress

(r.h.0; 30°C)

Count:	R:	R-squared:	Adj. R-squared:	RMS Residual:
16	.998	.997	.997	.092

Source	DF:	Sum Squares:	Mean Square:	F-test:
REGRESSION	1	36.662	36.662	4302.516
RESIDUAL (see fig.a)	14	.119	.009	p = .0001
TOTAL	15	36.781		

(r.h.55; 30°C)

Count:	R:	R-squared:	Adj. R-squared:	RMS Residual:
15	.995	.991	.99	.147

Source	DF:	Sum Squares:	Mean Square:	F-test:
REGRESSION	1	29.445	29.445	1356.272
RESIDUAL (see fig.b)	13	.282	.022	p = .0001
TOTAL	14	29.727		

(r.h.67; 3 0°C)

Count:	R:	R-squared:	Adj. R-squared:	RMS Residual:
15	.995	.991	.99	.147

Source	DF:	Sum Squares:	Mean Square:	F-test:
REGRESSION	1	36.417	36.417	1498.014
RESIDUAL	14	.34	.024	p = .0001
TOTAL	15	36.757		

(r.h.77; 30°C)

Count:	R:	R-squared:	Adj. R-squared:	RMS Residual:
16	.996	.992	.992	.142

Source	DF:	Sum Squares:	Mean Square:	F-test:
REGRESSION	1	35.58	35.58	1768.487
RESIDUAL	14	.282	.02	p = .0001
TOTAL	15	35.86		

(r.h.82; 30°C)

Count:	R:	R-squared:	Adj. R-squared:	RMS Residual:
16	.995	.99	.989	.177

Source	DF:	Sum Squares:	Mean Square:	F-test:
REGRESSION	1	41.806	41.806	1329.676

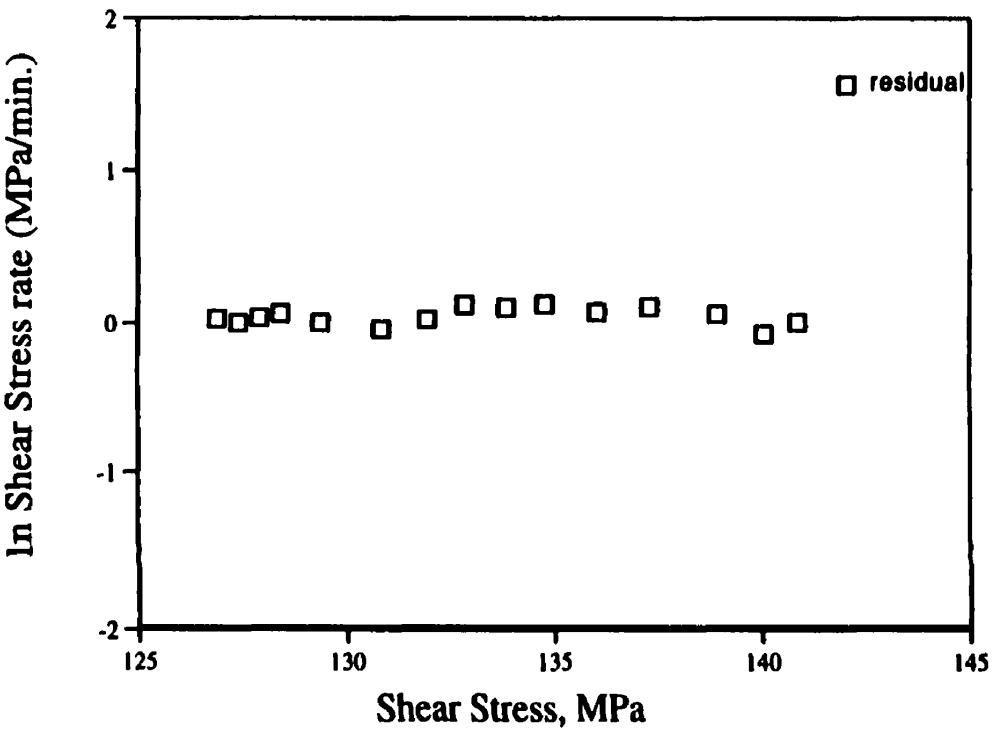

Fig a. Plot for the residual of ln (shear stress rate, MPa/s) versus shear stress and its fitted line obtained using linear model at r.h 0 and 30°C. The residual values are randomly scattered around 0 indicate that the fiting is accepted

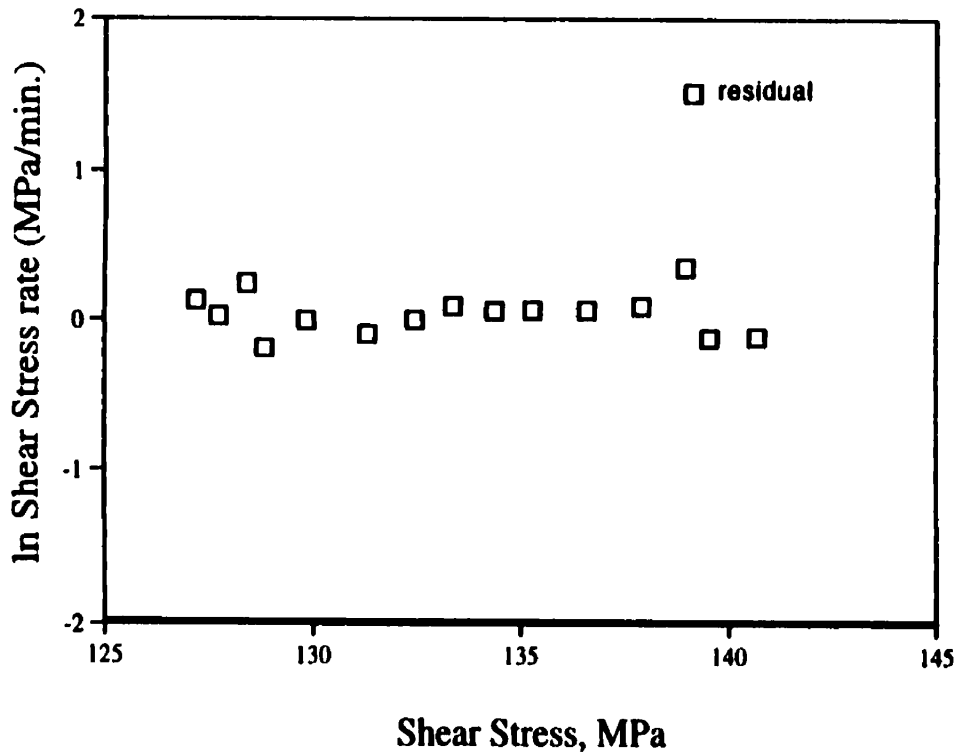

Fig.(b) Plot for the residual of ln (shear stress rate, MPa/s) versus shear stress and its fitted curve obtained using linear model at r.h 55 and 30°C. The residual values are randomly scattered around 0 indicate that the fiting is accepted

RESIDUAL	14	.44	.031	p = .0001
TOTAL	15	42.246		

(r.h.88; 30°C)

Count:	R:	R-squared:	Adj. R-squared:	RMS Residual:
16	.993	.985	.984	.175

Source	DF:	Sum Squares:	Mean Square:	F-test:
REGRESSION	1	28.939	28.939	940.983
RESIDUAL	14	.431	.031	p = .0001
TOTAL	15	29.369		

(r.h.0; 35°C)

Count:	R:	R-squared:	Adj. R-squared:	RMS Residual:
15	.998	.996	.996	.105

Source	DF:	Sum Squares:	Mean Square:	F-test:
REGRESSION	1	38.544	38.544	1731.23
RESIDUAL (see fig.c)	14	.312	.022	p = .0001
TOTAL	15	38.856		

(r.h.55; 35°C)

Count:	R:	R-squared:	Adj. R-squared:	RMS Residual:
16	.997	.994	.993	.124

Source	DF:	Sum Squares:	Mean Square:	F-test:
REGRESSION	1	33.888	33.888	2213.422
RESIDUAL (see fig.d)	14	.214	.015	p = .0001
TOTAL	15	34.103		

(r.h.67; 35°C)

Count:	R:	R-squared:	Adj. R-squared:	RMS Residual:
14	.996	.992	.991	.145

(r.h.67; 35°C)

Source	DF:	Sum Squares:	Mean Square:	F-test:
REGRESSION	1	38.082	38.082	1065.016
RESIDUAL	14	.501	.036	p = .0001
TOTAL	15	38.583		

(r.h.77; 35°C)

Count:	R:	R-squared:	Adj. R-squared:	RMS Residual:
15	.995	.99	.989	.167

Source	DF:	Sum Squares:	Mean Square:	F-test:
REGRESSION	1	38.582	38.582	1311.827

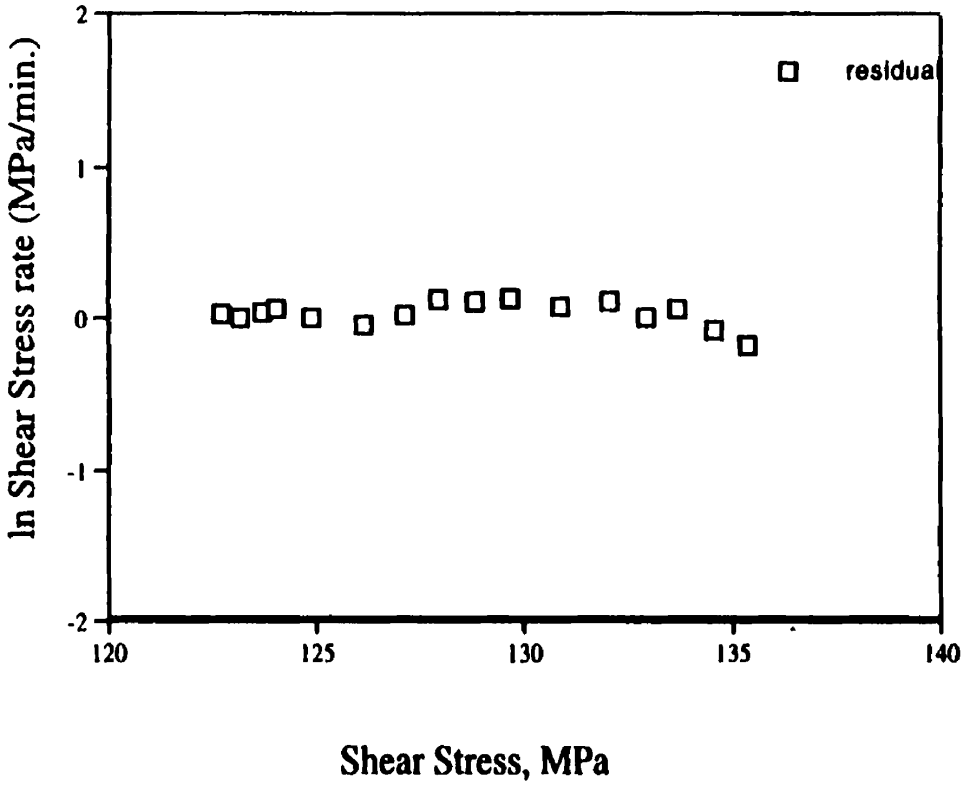

Fig.c. Plot for the residual of ln (shear stress rate, MPa/s) versus shear stress and its fitted line obtained using linear model at r.h 0 and 35°C. The residual values are randomly scattered indicate that the fiting is accepted

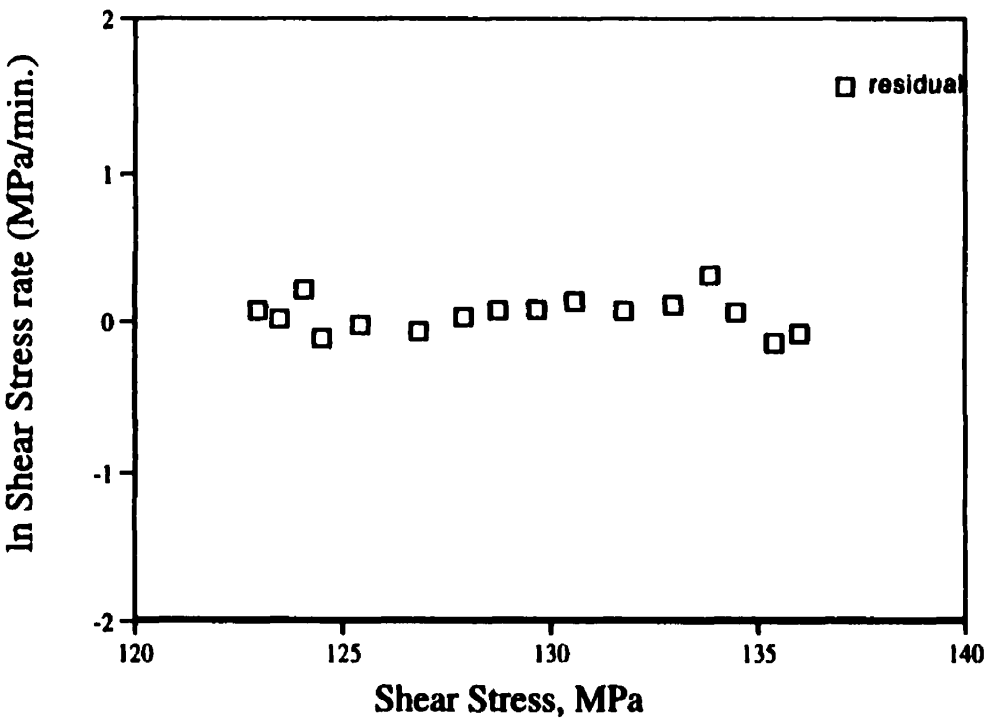

Fig.(d). Plot for the residual of ln (shear stress rate, MPa/s) versus shear stress and its fitted line obtained using linear model at r.h 55 and 35°C. The residual values are randomly scattered around 0 indicate that the fiting is accepted

RESIDUAL	14	.412	.029	p = .0001
TOTAL	15	38.994		

(r.h.82 35°C)

Count:	R:	R-squared:	Adj. R-squared:	RMS Residual:
13	.978	.956	.952	.402

Source	DF:	Sum Squares:	Mean Square:	F-test:
REGRESSION	1	45.8	45.8	229.661
RESIDUAL	12	2.393	.199	p = .0001
TOTAL	13	48.193		

(r.h.88; 35°C)

Count:	R:	R-squared:	Adj. R-squared:	RMS Residual:
15	.995	.991	.99	.145

Source	DF:	Sum Squares:	Mean Square:	F-test:
REGRESSION	1	30.571	30.571	527.284
RESIDUAL	14	.812	.058	p = .0001
TOTAL	15	31.383		

(r.h.0; 40°C)

Count:	R:	R-squared:	Adj. R-squared:	RMS Residual:
16	.996	.992	.991	.152

Source	DF:	Sum Squares:	Mean Square:	F-test:
REGRESSION	1	38.877	38.877	1692.983
RESIDUAL (see fig.e)	14	.321	.023	p = .0001
TOTAL	15	39.198		

(r.h.55; 40°C)

Count:	R:	R-squared:	Adj. R-squared:	RMS Residual:
14	.996	.992	.991	.14

Source	DF:	Sum Squares:	Mean Square:	F-test:
REGRESSION	1	28.175	28.175	1430.408
RESIDUAL(see fig.f)	12	.236	.02	p = .0001
TOTAL	13	28.412		

(r.h.67; 40°C)

Count:	R:	R-squared:	Adj. R-squared:	RMS Residual:
14	.993	.986	.985	.199

Source	DF:	Sum Squares:	Mean Square:	F-test:
REGRESSION	1	42.911	42.911	429.055
RESIDUAL	14	1.4	.1	p = .0001
TOTAL	15	44.311		

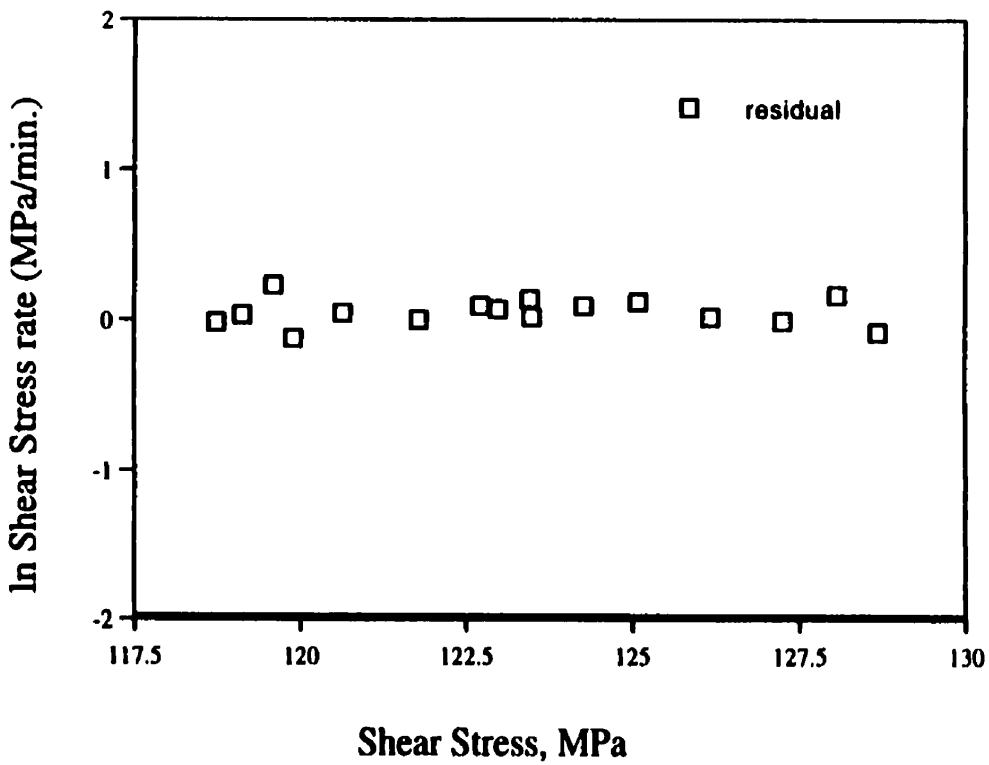

Fig.(c). Plot for the residual of ln (shear stress rate, MPa/s) versus shear stress and its fitted line obtained using linear model at r.h 0 and 40°C. The residual values are randomly scattered around 0 indicate that the fiting is accepted

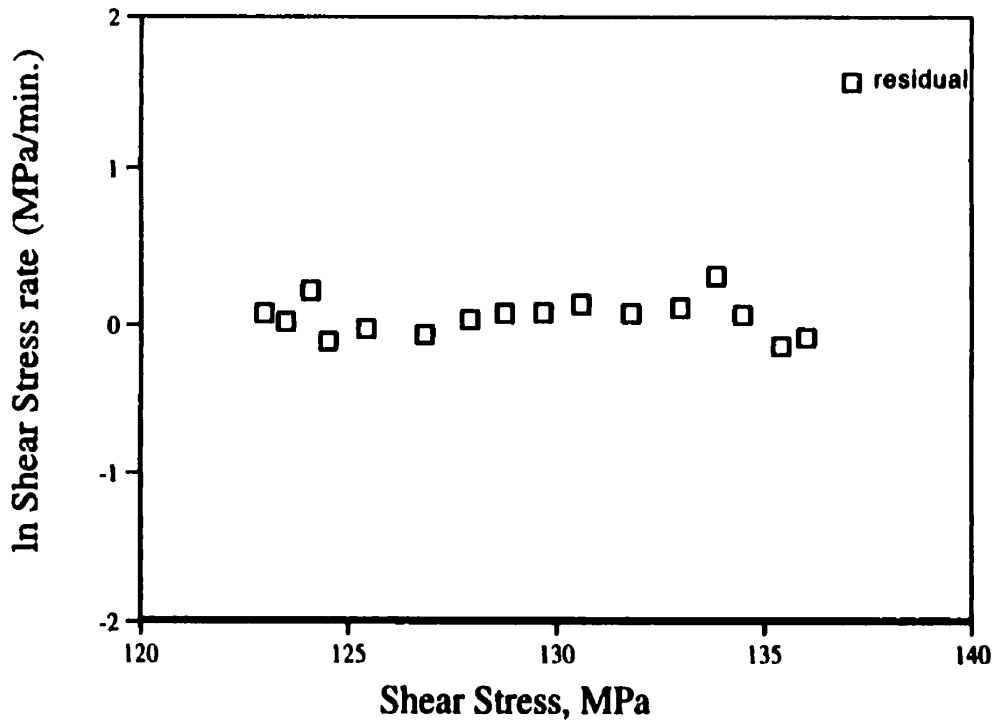

Fig.(f). Plot for the residual of ln (shear stress rate, MPa/s) versus shear stress and its fitted line obtained using linear model at r.h 55 and40°C. The residual values are randomly scattered around 0 indicate that the fiting is accepted

(r.h.77; 40°C)

Count:	R:	R-squared:	Adj. R-squared:	RMS Residual:
14	.991	.981	.98	.236

Source	DF:	Sum Squares:	Mean Square:	F-test:
REGRESSION	1	47.082	47.082	507.927
RESIDUAL	14	1.298	.093	p = .0001
TOTAL	15	48.38		

(r.h.82; 40°C)

Count:	R:	R-squared:	Adj. R-squared:	RMS Residual:
15	.959	.92	.914	.607

Source	DF:	Sum Squares:	Mean Square:	F-test:
REGRESSION	1	61.451	61.451	175.579
RESIDUAL (see fig.g)	14	4.9	.35	p = .0001
TOTAL	15	66.35		

(r.h.88; 40°C)

Count:	R:	R-squared:	Adj. R-squared:	RMS Residual:
15	.959	.92	.914	.607

Source	DF:	Sum Squares:	Mean Square:	F-test:
REGRESSION	1	31.831	31.831	940.987
RESIDUAL (see fig.h)	14	.474	.034	p = .0001
TOTAL	15	32.305		

(r.h.0; 45°C)

Count:	R:	R-squared:	Adj. R-squared:	RMS Residual:
12	.995	.991	.99	.143

Source	DF:	Sum Squares:	Mean Square:	F-test:
REGRESSION	1	32.727	32.727	1389.121
RESIDUAL	12	.283	.024	p = .0001
TOTAL	13	33.009		

(r.h.55; 45°C)

Count:	R:	R-squared:	Adj. R-squared:	RMS Residual:
12	.995	.989	.988	.179

Source	DF:	Sum Squares:	Mean Square:	F-test:
REGRESSION	1	29.478	29.478	895.289
RESIDUAL	12	.395	.033	p = .0001
TOTAL	13	29.873		

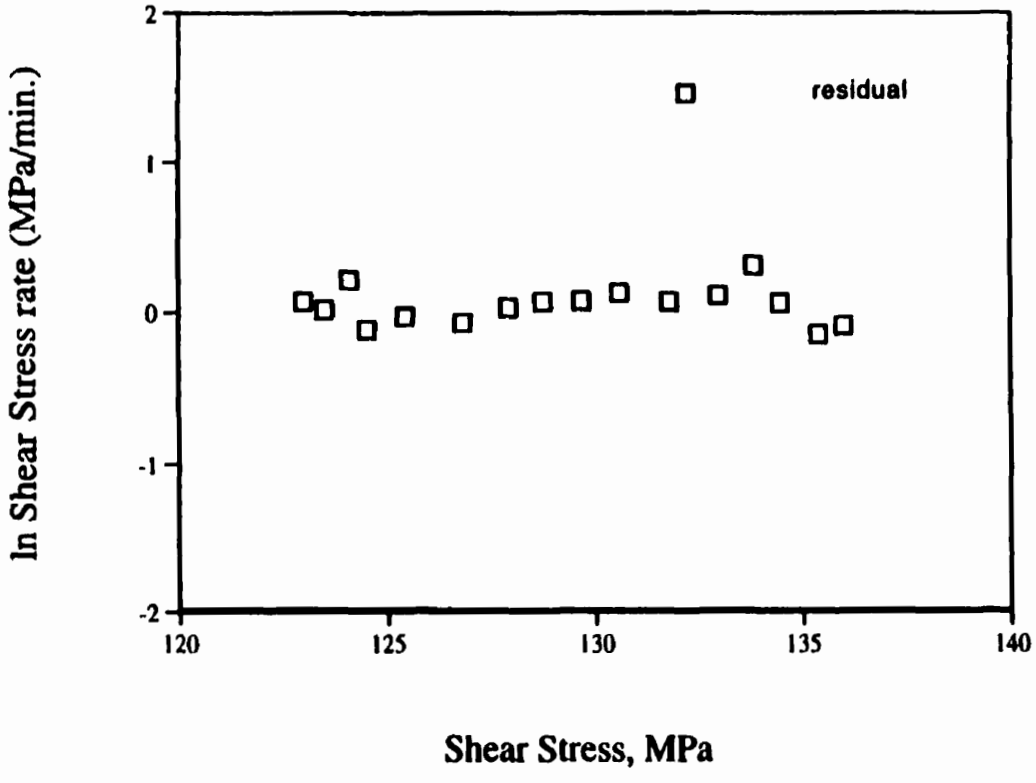

Fig.(g). Plot for the residual of ln (shear stress rate, MPa/s) versus shear stress and its fitted line obtained using linear model at r.h 0 and45°C. The residual values are randomly scattered around 0 indicate that the fiting is accepted

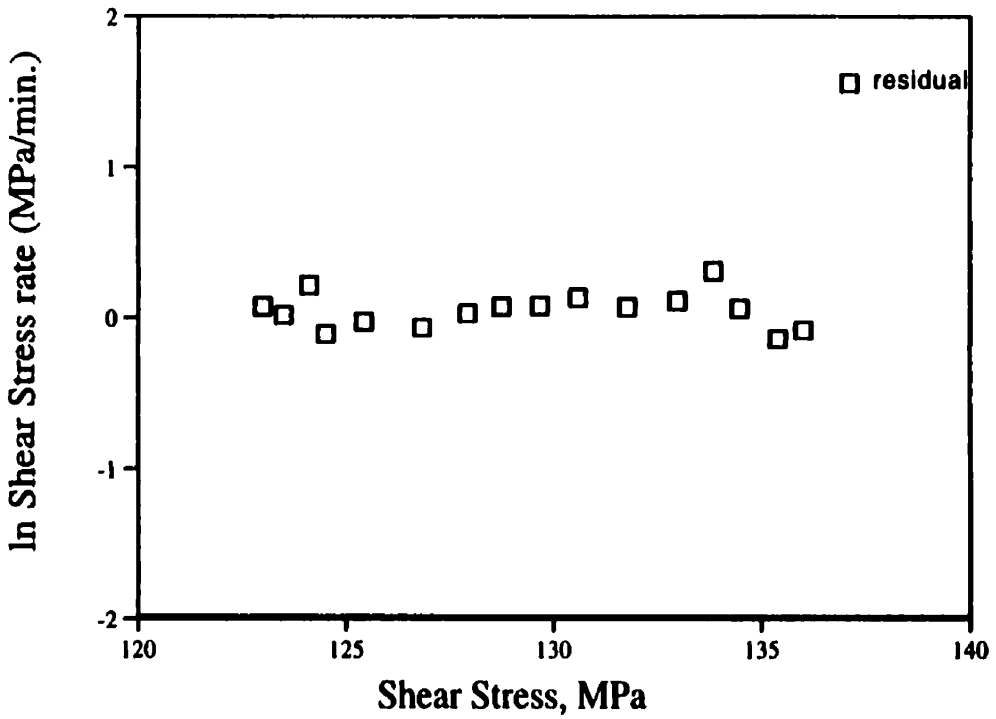

Fig.(h). Plot for the residual of ln (shear stress rate, MPa/s) versus shear stress and its fitted line obtained using linear model at r.h 55 and45°C. The residual values are randomly scattered around 0 indicate that the fiting is accepted

(r.h.67; 45°C)

Count:	R:	R-squared:	Adj. R-squared:	RMS Residual:
12	.99	.98	.978	.22

Source	DF:	Sum Squares:	Mean Square:	F-test:
REGRESSION	1	28.387	28.387	269.458
RESIDUAL	13	1.37	.105	p = .0001
TOTAL	14	29.757		

(r.h.77; 45°C)

Count:	R:	R-squared:	Adj. R-squared:	RMS Residual:
13	.988	.977	.975	.262

Source	DF:	Sum Squares:	Mean Square:	F-test:
REGRESSION	1	48.792	48.792	725.61
RESIDUAL	13	.874	.067	p = .0001
TOTAL	14	49.667		

(r.h.82; 45°C)

Count:	R:	R-squared:	Adj. R-squared:	RMS Residual:
13	.974	.948	.944	.423

Source	DF:	Sum Squares:	Mean Square:	F-test:
REGRESSION	1	30.106	30.106	558.151
RESIDUAL	13	.701	.054	p = .0001
TOTAL	14	30.808		

(r.h.88; 45°C)

Count:	R:	R-squared:	Adj. R-squared:	RMS Residual:
15	.997	.993	.993	.127

Source	DF:	Sum Squares:	Mean Square:	F-test:
REGRESSION	1	30.597	30.597	1888.594
RESIDUAL	13	.211	.016	p = .0001
TOTAL	14	30.808		

Appendix II

Deformation kinetic data for evaluation of sucrose activation energy at maximum loads 4.5 KN

R.H.	Temp.	Equation of Strain vs Avg Strs	Arrhenius plot slope		
0%	303K	y = .33x - 41.35, r2 = .997	y = -27529.024x + 90.747, r2 = .998		
0%	308K	y = .38x - 46.72, r2 = .996			
0%	313K	y = .41x - 48.32, r2 = .992			
0%	318K	y = .47x - 55.00, r2 = .991			
55%	303K	y = .318x-39.89, r2 = .995	y = -24438.382x + 80.482, r2 = .994		
55%	308K	y = .337x - 40.952, r2 = .994			
55%	313K	y = .421x-50.41, r2 = .992			
55%	318K	y = .451x - 52.507, r2 = .993			
67%	303K	y = .390x - 46.72, r2 = .996,	y = -50399.284x + 177.545, r2 = .989		
67%	308K	y = .397x - 45.158, r2 = .994			
67%	313K	y = .387x - 41.466, r2 = .997			
67%	318K	y = .393x - 40.095, r2 = .991			
77%	303K	y = .338x - 39.824, r2 = .992	y = -63553.792x + 220.248, r2 = .966		
77%	308K	y = .306x - 32.724, r2 = .994,			
77%	313K	y = .360x - 36.429, r2 = .994			
77%	318K	y = .573x - 55.513, r2 = .991			
82%	303K	y = .34x - 38.25, r2 = .99	y = -75430.759x + 262.499, r2 = .936		
82%	308K	y = .449x - 47.964, r2 = .993			
82%	313K	y = .476x - 51.046, r2 = .989			
82%	318K	y = .45x - 42.028, r2 = .98,			